

## LOW-PRESSURE DIFFERENTIATION OF MELANEPHELINITIC MAGMA AND THE ORIGIN OF IJOLITE PEGMATITES AT LA MADERA, CÓRDOBA, ARGENTINA

MIGUEL ANGEL GALLISKI<sup>§</sup>

*Laboratorio de Mineralogía y Geoquímica, IANIGLA – CRICYT – CONICET, Avda. A. Ruiz Leal s/n Parque Gral.  
San Martín, CC330, 5500 Mendoza, Argentina*

RAÚL LIRA

*CONICET, Museo de Mineralogía y Geología “Dr. Alfredo Stelzner”, Facultad de Ciencias Exactas,  
Físicas y Naturales, Universidad Nacional de Córdoba, Avda. Vélez Sarsfield 299, 5000, Córdoba, Argentina*

MICHAEL J. DORAIS

*Department of Geology, Brigham Young University, Provo, Utah 84602–4606, U.S.A.*

### ABSTRACT

The ijolitic pegmatites of La Madera are exposed in a quarry in Córdoba, Argentina. They occur as dykelets and dykes 0.2 to 0.5 m wide and 5 to 20 m in length, emplaced in a volcanic olivine melanephelinite of probable Late Cretaceous age. The dykes are composed of pyroxene, nepheline, analcime, devitrified glass, magnetite, phillipsite-Na, magnesiokatophorite, eckermannite, biotite, calcite and chlorite. The pyroxene is strongly zoned, with compositions grouped about four different Mg# values (80, 70, 55 and 20), showing a segmented trend of increasing alkalinity from diopside to aegirine-rich aegirine-augite. Nepheline ( $\text{Ne}_{66}\text{Ks}_{31}\text{Qtz}_3$ ) is locally replaced by zeolites in the more leucocratic dykes. Idiomorphic analcime is a locally important hydrous phase, that is invariably replaced by phillipsite-Na. Apatite and perovskite are REE- and especially Sr-enriched minerals. The devitrified glass of the mesostasis contains amygdules that are, in places, squeezed between crystals and mesostasis. The amygdules are composed dominantly of phillipsite-Na, with small quantities of calcite, and scarce chlorite, apatite and Fe-oxides, with textural relationships suggesting formation by liquid immiscibility. Textural relationships and whole-rock compositions show that the ijolitic pegmatites were formed by  $\text{H}_2\text{O}$ -undersaturated,  $\text{P}_2\text{O}_5$ -,  $\text{CO}_2$ - and incompatible-element-bearing melts that were derived by fractional crystallization of a parent olivine melanephelinite. The pegmatite-forming melt was collected and transported upward by diapiric transfer of low-density melt fractions; transport occurred in discrete units now represented by scattered segregation vesicles. These melts were emplaced and crystallized in the irregular fractures of the consolidated upper levels of the lava flow. During this process, the residual pegmatite-forming melt evolved until two immiscible fractions began to separate. One melt that led to the formation of phillipsite-Na amygdules, resembles nepheline syenite in its major-element composition. The other is represented by a more basic dark glass, K-, Fe-, Mg-, and P-enriched, and Na-, Al- and Ca-depleted compared to the leucocratic fraction.

*Keywords:* ijolitic pegmatites, melanephelinite, liquid immiscibility, analytical data, isotopic data, La Madera, Argentina.

### SOMMAIRE

Nous avons étudié les pegmatites ijolitiques de La Madera, qui affleurent dans une carrière à Córdoba, en Argentine. Elles se présentent en filonnets et en filons allant de 0.2 à 0.5 m en largeur et de 5 à 20 m en longueur, mises en place dans une mélanéphéline volcanique à olivine, probablement d'âge crétaïc tardif. Les filons sont composés de pyroxène, néphéline, analcime, verre dévitrifié, magnétite, phillipsite-Na, magnésiokatophorite, eckermannite, biotite, calcite et chlorite. Le pyroxène est fortement zoné, les compositions regroupées selon quatre intervalles distincts de valeurs de Mg# (80, 70, 55 et 20), montrant une augmentation discontinue en alcalinité le long de la lignée diopside à aegirine-augite sodique. La néphéline ( $\text{Ne}_{66}\text{Ks}_{31}\text{Qtz}_3$ ) est localement remplacée par des zéolites dans les filons plutôt leucocrates. L'analcime en cristaux idiomorphes est une phase hydratée localement importante, mais qui se voit remplacée par la phillipsite-Na. L'apatite et la pérovskite sont enrichies en terres rares et surtout en Sr. Le verre dévitrifié de la pâte contient des amygdules qui semblent par endroits avoir été serrés entre cristaux et la pâte. Ces amygdules sont faites surtout de phillipsite-Na, avec de petites quantités de calcite, et ainsi que chlorite, apatite et

<sup>§</sup> E-mail address: galliski@lab.cricyt.edu.ar

oxydes de fer plus rares, les relations texturales nous poussant à proposer une origine par immiscibilité liquide. Les relations texturales et les compositions globales montrent que les pegmatites ijolitiques se sont formées à partir de magmas sous-saturés en  $H_2O$ , et porteurs de  $P_2O_5$ ,  $CO_2$  et d'éléments incompatibles, dérivés par cristallisation fractionnée d'une mélanéphéline parentale à olivine. Le magma qui cristallise sous forme de pegmatite s'est concentré et a été transporté vers le haut par transfert diapirique de fractions de magma à faible densité; le transfert s'est effectué en volumes distincts représentés maintenant par des ségrégations éparses. Ces volumes de magma ont été mis en place et ont cristallisé le long de fractures irrégulières dans les parties supérieures de la coulée de lave. Au cours de ce processus, le magma a continué d'évoluer jusqu'au point où deux fractions immiscibles se sont formées. Un liquide a donné la phillipsite-Na en amygdules, ressemblant à une syénite néphélinique dans sa composition globale. L'autre serait représenté par un verre foncé, enrichi en K, Fe, Mg, et P, et appauvri en Na, Al et Ca par rapport à la fraction leucocrate.

(Traduit par la Rédaction)

**Mots-clés:** pegmatites ijolitiques, mélanéphéline, immiscibilité liquide, données analytiques, données isotopiques, La Madera, Argentine.

## INTRODUCTION

The development of the pegmatitic texture in granitic pegmatites has generally been associated with magmatic crystallization of volatile-saturated melts in the presence of an aqueous fluid phase. This interpretation was based on the experimental results obtained by Jahns & Burnham (1969). Nevertheless, more recent experiments have focused on the inhibition of nucleation of crystals and their growth in disequilibrium conditions (Fenn 1977, London 1992). The appropriate conditions to promote these effects would be found in initially  $H_2O$ -undersaturated granitic melts enriched in volatile elements (Li, F, B, P) (London *et al.* 1989, London 1992).

Data are sparse for more basic magmas, though pegmatitic segregations in basalts have been described (Kuno *et al.* 1957, Kuno 1965, Greenough & Dostal 1992, Puffer & Horter 1993). Some descriptions of ijolitic pegmatites have been published (*e.g.*, Rankin & Le Bas 1974, Kogarko 1990). Galliski *et al.* (1992) described pegmatitic dykes of ijolite composition in nephelinitic rocks and supported the idea that they crystallized at very low pressures and presumably at a high rate of cooling. This circumstance and the fact that Bailey & Hampton (1990) showed that  $CO_2$  prevails over  $H_2O$  in magmas of this composition provided us with an opportunity to explore the hypothesis of disequilibrium crystallization in a context of low-pressure fractionation of an alkaline basic melt. We also investigated the possibility that such a magma might undergo immiscibility at low pressures. Such a process has been invoked at higher pressures to explain the origin of the nephelinite – ijolite – carbonatite association (Koster van Groos & Wyllie 1968, Rankin & Le Bas 1974, Le Bas 1977, Kjarsgaard & Hamilton 1988, Wyllie *et al.* 1990). Our investigation focuses on the occurrence of such rocks at La Madera, Córdoba, Argentina, and involves detailed petrographic work, whole-rock geochemistry of representative lithologies, mineral identification and chemistry, and stable isotope considerations of the origin of liquids and fluids.

## GEOLOGICAL SETTING AND PETROGRAPHY

La Madera is a small hill situated at  $33^{\circ}39' S$ ,  $65^{\circ}01' W$ , close to Chaján, province of Córdoba, Argentina (Fig. 1). The hill is one of six small remnants of volcanic edifices that outcrop in the surrounding loess plains known as "pampa". The rocks are olivine melane-nphelinites; the abundant references in the regional geological literature have been reviewed by Galliski & Lira (1991). López & Solá (1981) described the petrography of the four best known occurrences and published two whole-rock K–Ar dates,  $75 \pm 5$  Ma and  $66 \pm 5$  Ma, for La Garrapata and La Leoncita hills, respectively, which

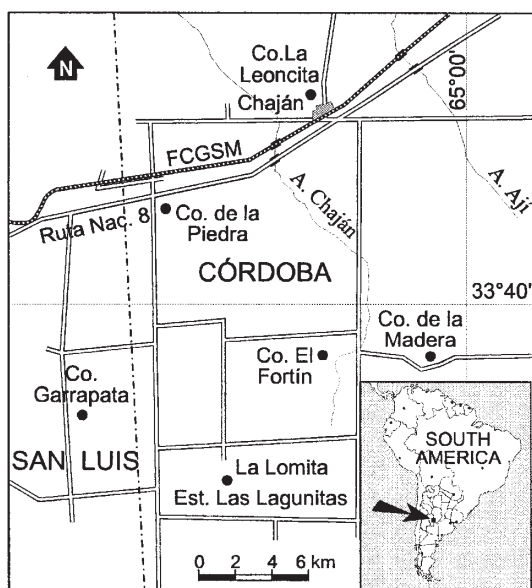


FIG. 1. Location map of the ijolite pegmatites at La Madera, Córdoba, Argentina.

place the timing of magmatism in the Upper Cretaceous. Galliski *et al.* (1992) documented the morphology and petrography of the ijolitic pegmatites in the walls of a ballast quarry located at La Madera.

The melanephelinite at the La Madera quarry is a greenish to dark gray rock found in layers defined by subhorizontal jointing. The melanephelinite is microphyritic, with phenocrysts of fractured olivine partially altered to clinoclere and iron oxides, contained in an aphanitic matrix. The groundmass is holocrystalline and contains pyroxene, nepheline, analcime, magnetite, perovskite and biotite. Occasionally, small restricted domains show an enrichment in nepheline, analcime, biotite and zeolites. The rock shows local evidence of having undergone a possibly late-magmatic or slight metasomatic overprint, with the development of a second generation of poikilitic pyroxene, biotite, nepheline and zeolites. The rock has abundant, empty millimetric cavities that are dispersed throughout and are of ellipsoidal or irregular geometry. Dispersed in the foidite, there are lighter-colored ovoid enclaves 5 to 20 cm long consisting of zeolites and minor aegirine. Randomly distributed ellipsoidal (1 to 4 cm) segregation vesicles (*e.g.*, Anderson *et al.* 1984) are more frequent. These contain borders of phenocrystic analcime that is in some cases replaced by phillipsite-Na. Internally radiating clinopyroxene and apatite are contained in a cracked glass matrix whose modal abundance increases toward the center. More leucocratic segregation vesicles have a less regular geometry and are completely crystallized. Their cores consist of a late-stage zeolitic phase, generally phillipsite-Na.

In the eastern wall of the quarry, the melanephelinite is cut by several irregular dykes and dykelets with a well-defined pegmatitic fabric (Fig. 2). These ijolitic pegmatites are generally tabular to lenticular, ranging from a few centimeters up to more than 20 m in length and varying from 0.01 to 1 m in thickness, with an average between 0.2 to 0.5 m. They were emplaced without a regular structural control, and it is difficult to define strikes and dips. The dykes in the quarry wall vary from subvertical to subhorizontal and show frequent changes in orientation. The contacts between the host rocks and the dykes are usually sharp and straight, but some pinching and swelling of the dykes are present. The contact is continuous, in some cases solely marked by a bleached band with a greenish hue due to the strongly chloritized olivine of the melanephelinite; this band can reach 0.05 m in width, depending on the thickness of the dyke.

There are two varieties of dyke in the quarry: melanocratic dykes consisting of predominantly pyroxene, nepheline, analcime and a greenish red groundmass (Fig. 3A), and leucocratic dykes with pyroxene, replaced nepheline, zeolites and calcite (Fig. 3B). Both types show mineralogical and textural zoning that is in some cases asymmetrical (Fig. 3C). The textural zoning is defined by a border zone parallel to the contact that usu-

ally has a comb texture defined by nepheline and pyroxene. The wall zone may show a subdivergent arrangement of pyroxene prisms similar to a comb texture with interstices filled with other minerals and groundmass. In the melanocratic dykes, there are mm-size amygdules, in some cases irregularly shaped, seemingly squeezed between adjacent crystals (Fig. 3D). The amygdules are filled with zeolites that give an *ocellus-like* texture. The cores of the thicker dykes are richer in zeolites and occasionally present drusy vugs with idiomorphic zeolites and minor calcite. Dykes with compositions intermediate between the melanocratic and leucocratic rocks dykes are more reddish in color, nepheline is almost completely replaced by phillipsite-Na, and goethite and chlorite are dispersed.

The analytical work was performed on samples of the most accessible and representative fresh dykes, labeled 1, 2, 3, 5, and 7 in correlative order from north to south. Dyke 1 is thin and becomes progressively wider toward the upper levels until it reaches 20 cm in thickness. It is melanocratic and has large, tabular crystals of pyroxene, nepheline prisms and zeolite amygdules of irregular distribution in a central brown groundmass. The thickness of dyke 2 varies from 15 to 50 cm where it lies subhorizontally. It is dark and has accumulations of analcime and zeolites at the top. Dyke 3 is almost 40 cm thick and is subvertical; it is characterized by brown nepheline partially replaced by zeolites. At location 5, there are two subhorizontal dykes with an average thickness of 1 m each. The lower dyke is melanocratic, and the upper is leucocratic, in which nepheline is replaced by zeolites (Fig. 3B). Dyke 7 is 30 cm thick; it is melanocratic and is partially altered.

#### EXPERIMENTAL METHODS

The host olivine melanephelinite and melanocratic and leucocratic dykes were analyzed for major and trace elements by X-ray fluorescence, instrumental neutron activation, and inductively coupled plasma techniques of analysis by XRAL Activation Services Incorporated. The results are presented in Table 1. Polished thin sections of the dykes were analyzed with a CAMECA SX-50 electron microprobe in the Department of Geological Sciences, Indiana University. Operating conditions were 15 kV for all minerals, 20 nA and 1–2  $\mu\text{m}$  of beam size for pyroxene, amphibole, magnetite and perovskite, and 15 nA and 10  $\mu\text{m}$  beam size for nepheline, apatite, glass and zeolites. Natural minerals were used as standards, and the data were reduced using the procedures of Pouchou & Pichoir (1985). The results are presented in Tables 2 to 9.

Oxygen from silicates and oxides was extracted following the fluorination technique of Clayton & Mayeda (1963) using  $\text{BrF}_3$  as a reactant in nickel bombs at temperatures from 550° to 600°C. A  $\text{CO}_2$  fraction was collected after conversion of  $\text{O}_2$  over a heated graphite disc.  $\text{CO}_2$  from calcite found in the vugs was collected after



FIG. 2. The thickest dyke of melanocratic ijolitic pegmatite outcrop in the wall of the quarry.

FIG. 3. (A) Melanocratic ijolitic pegmatite emplaced in melanephelinite showing the pyroxene + nepheline + analcite + groundmass association containing amygdules of phillipsite-Na. Magnifier in the lower right corner is 5 cm long. (B) Leucocratic zeolite-bearing ijolitic pegmatite showing a discolored, partially chloritized fringe, in the melanephelinite host-rock. The dominant assemblage comprises pyroxene + nepheline + phillipsite-Na; the picture was rotated 90° clockwise. (C) Contact between melanephelinite and ijolitic pegmatite. Note the millimetric nepheline-dominant border-zone that passes transitionally to a wall zone by an increase in the number of pyroxene crystals contained in a nepheline-dominant mesostasis. The wall zone grades into the intermediate zone, where the spaces between comb-textured long prisms of diopside and partially replaced nepheline are filled by phillipsite-Na. (D) Polished section of a melanocratic ijolitic pegmatite showing idiomorphic crystals of nepheline (Ne) in contact with deformed amygdules of phillipsite-Na (Ph-Na) contained in a dark groundmass (Grd). (E) Photomicrograph of a thin section under plane-polarized light of a melanocratic ijolitic pegmatite showing tabular prisms of pyroxene (Cpx) with alkali-richer borders, idiomorphic acicular apatite (Ap), sub- to idiomorphic perovskite (Prv), interstitial brown groundmass (Grd), and phillipsite-Na (Ph-Na). Note that the brown groundmass contains, in the center, a deformed amygdule of phillipsite-Na showing between them clear textural patterns of contact between two immiscible liquids; in the bottom left quarter are included tiny microlites of amphibole. (F) Thin section in plane light showing triangular interstitial filling of slightly devitrified groundmass (Grd) containing idiomorphic crystals of apatite (Ap). The limits of the groundmass are prisms of pyroxene (Cpx) and one amygdule of phillipsite-Na (Ph-Na) showing liquid-state deformation at the contact with apatite. Note the abundant crystals of apatite in the brown groundmass. (G) Segregation vesicles contained in melanephelinite showing a border zone formed by pyroxene + apatite that grades into greenish idiomorphic crystals of analcime included in a brown, glassy groundmass with skeletal crystals of opaque minerals. (H) Thin-section view with plane-polarized light of the contact between the enclosing melanephelinite (immediately to the left, out of field of view) and one segregation vesicle showing, from left to right, a concentric halo of clinopyroxene crystals that passes to a brown mesostasis, and further, to a corona of idiomorphic crystals of analcime replaced by phillipsite-Na.

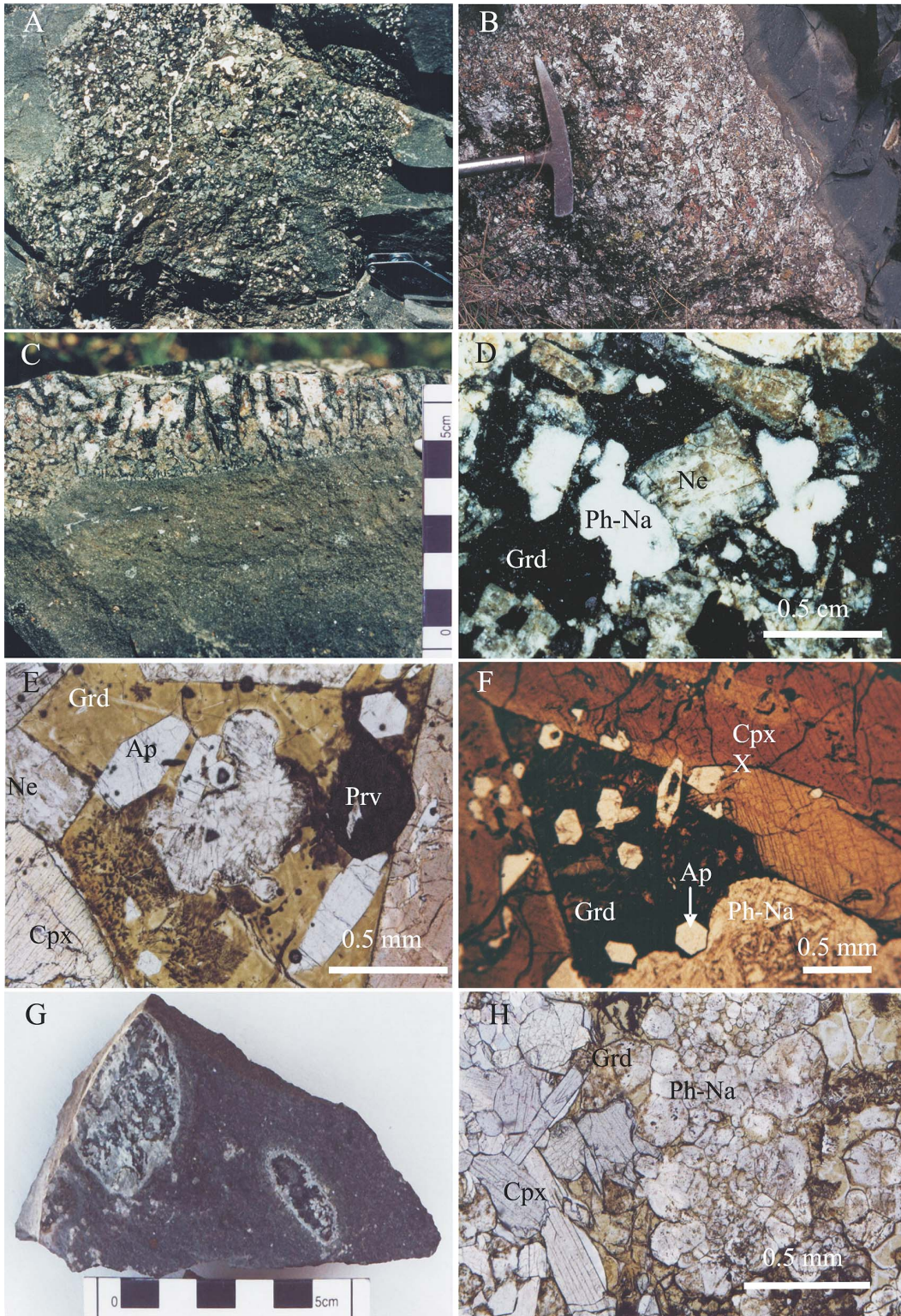


TABLE 1. CHEMICAL ANALYSIS OF MAIN ROCKS FROM LA MADERA

Sample	LM07	LM08	LM09	Cont.	LM07	LM08	LM09
SiO <sub>2</sub> (Wt %)	39.80	40.30	40.30	As	0.5	1	1
TiO <sub>2</sub>	3.07	3.38	2.91	Se	1	1	1
Al <sub>2</sub> O <sub>3</sub>	9.23	15.70	14.30	Sb	0.05	0.2	0.05
Fe <sub>2</sub> O <sub>3</sub>	11.20	8.90	8.27	Ag	0.4	0.4	0.4
MnO	0.16	0.11	0.11	Rb	55	44	70
MgO	13.20	5.45	5.13	Cs	1	0.9	1.5
CaO	11.00	10.30	12.10	Ba	890	1700	1500
Na <sub>2</sub> O	2.89	5.48	2.60	Sr	1980	2440	2420
K <sub>2</sub> O	3.10	3.49	3.03	Ta	9.9	8.2	6.8
P <sub>2</sub> O <sub>5</sub>	1.22	1.56	2.07	Nb	170	220	180
CO <sub>2</sub>	0.12	0.25	0.15	Hf	10	13	7.8
LOI	0.62	3.00	7.54	Zr	430	630	330
Total	95.61	97.92	98.51	Y	20	30	20
Mg#	70.0	54.8	55.1	Th	8.6	4.8	3
				U	2.7	3.4	3.7
Cr (ppm)	400	10	5	La	119	115	85.2
Ni	330	60	50	Ce	232	210	117
Co	60	28	28	Nd	95	88	44
Sc	17	10	7	Sm	16.9	14.3	8.71
V	160	210	200	Eu	5.32	5.4	3.66
Cu	41	71	65	Tb	1.2	1.1	0.9
Pb	3	6	2	Yb	1.8	1.86	1.6
Zn	130	130	99	Lu	0.23	0.24	0.2
Cd	2	2	2	Br	2.7	2.4	2.8
W	2	2	1	B	5	10	20
Mo	1	1	1	Be	5	7	4

References: LM07 olivine melanephelinite, LM08 ijolite pegmatite, LM09 zeolite-bearing ijolite pegmatite

overnight reaction of the sample with 103% phosphoric acid at 50°C following the method of Rosenbaum & Sheppard (1986). Oxygen and carbon isotope ratios were measured in a Finnigan Mat mass spectrometer. Carbon and oxygen values in ‰ are related to PDB and SMOW standards, respectively. Analyses were run at the Stable Isotope Lab of the Department of Geological Sciences of Indiana University.

## RESULTS

### Geochemistry

The host rock of La Madera ijolitic pegmatites is an alkaline rock (Table 1). Following the IUGS nomenclature (Le Maitre 2002), and on the basis of the normative nepheline (12.86%) and MgO (13.2%) contents, we classify the rock as an olivine melanephelinite. Compared to the mean chemical composition of olivine melanephelinites given by Le Bas (1989, Table 4), the La Madera olivine melanephelinite is slightly poorer in Al, Fe(t), Ca and Na, and richer in K and P.

The dykes of melanocratic ijolitic pegmatite have compositions similar to that of the parental volcanic host, but are enriched in Ti, Al, alkalis and P and are considerably depleted in Mg and less so in Fe. The ijolite

dykes with zeolites show chemical compositions similar to those lacking zeolites in terms of major elements, but are slightly richer in Ca and P.

The *spider* diagram (Fig. 4) shows that the ijolitic pegmatites, in relation to the olivine melanephelinite, are comparatively richer in Sr, Ba, K, Nb, P, Zr, Hf and poorer in Th, Ta, Ce, Sm and Sc. The zeolite-bearing ijolitic pegmatites are rich in Ba, Rb and P, and depleted in Th, La and Ce compared to the pegmatites lacking zeolites. They are also notably depleted in Nd and less depleted in Sm, Zr and Hf. Compared to the host olivine melanephelinite, Rb is enriched in the leucocratic pegmatitic dykes, whereas Zr and Hf are depleted, and the melanocratic pegmatite dykes show the opposite trends.

## CHEMICAL COMPOSITION OF THE MINERALS

### Clinopyroxene

Clinopyroxene occurs as euhedral crystals that reach 5 cm length. Crystals are tabular and zoned and exhibit good development of {110} and {010} crystallographic forms. Some crystals that grew in the groundmass are skeletal and partially hollow. Three groups of compositions (Table 2) correspond to diopside, aegirine-augite,

TABLE 2. REPRESENTATIVE COMPOSITIONS OF PYROXENE FROM IJOLITE PEGMATITES, LA MADERA SUITE, ARGENTINA

Sample	MP 341c	MP 341r	MP 342c	MP 342r	MP 342r	MP 342rr	MP 342r	MP 342r	MP 342i	MP 342c	MP 343c	MP 343r	MP 343i	MP 343i	MP 751c	MP 751c
	4	5	10	11	12	13	14	15	16	17	18	19	20	21	22	23
SiO <sub>2</sub> wt.%	48.42	50.78	50.83	51.28	50.12	50.85	51.04	50.08	50.89	50.51	52.13	50.96	51.18	52.49	49.05	48.89
TiO <sub>2</sub>	3.04	1.96	1.62	1.81	1.96	1.72	4.59	5.95	1.48	1.65	1.22	2.41	2.67	1.18	2.37	2.53
Al <sub>2</sub> O <sub>3</sub>	3.06	1.39	1.09	0.57	0.54	0.61	0.50	0.46	1.00	1.06	0.52	0.69	0.66	0.54	2.38	2.48
Fe <sub>2</sub> O <sub>3</sub>	4.11	3.07	3.43	4.63	5.95	4.54	19.51	18.52	4.03	3.91	2.27	4.36	5.11	2.23	4.48	4.38
MgO	13.28	14.13	14.61	11.90	11.63	11.85	2.380	2.68	14.80	14.58	14.48	11.41	10.86	14.58	14.04	13.97
CaO	23.88	23.89	24.31	21.45	21.40	21.53	2.52	2.92	24.32	24.32	23.86	20.38	19.71	24.03	24.09	24.21
MnO	0.10	0.09	0.13	0.14	0.15	0.21	0.19	0.19	0.12	0.11	0.14	0.12	0.18	0.15	0.12	0.05
FeO	2.82	3.28	2.32	5.61	4.45	5.23	4.76	4.29	1.75	1.95	4.00	6.21	6.28	3.87	1.69	1.81
Na <sub>2</sub> O	0.75	0.71	0.56	1.83	1.93	1.77	11.38	11.26	0.60	0.58	0.63	2.23	2.70	0.65	0.67	0.64
Total	99.46	99.30	98.90	99.22	98.13	98.31	96.87	96.35	98.99	98.67	99.25	98.77	99.35	99.72	98.89	98.96
Si <i>apfu</i>	1.816	1.897	1.902	1.937	1.918	1.937	1.998	1.969	1.901	1.896	1.945	1.935	1.936	1.947	1.841	1.835
<sup>[4]</sup> Al	0.135	0.061	0.048	0.026	0.024	0.028	0.002	0.021	0.044	0.047	0.023	0.031	0.029	0.024	0.105	0.110
Fe <sup>3+</sup>	0.049	0.042	0.049	0.037	0.058	0.035	0.000	0.010	0.055	0.057	0.032	0.034	0.035	0.029	0.053	0.055
ΣT	2.000	2.000	2.000	2.000	2.000	2.000	2.000	2.000	2.000	2.000	2.000	2.000	2.000	2.000	2.000	2.000
<sup>[6]</sup> Al							0.021									
Fe <sup>2+</sup>	0.067	0.045	0.047	0.094	0.113	0.095	0.575	0.538	0.059	0.053	0.032	0.091	0.111	0.033	0.073	0.069
Ti	0.086	0.055	0.046	0.051	0.056	0.049	0.135	0.176	0.042	0.047	0.034	0.069	0.076	0.033	0.067	0.071
Mg	0.742	0.787	0.815	0.670	0.663	0.673	0.139	0.157	0.824	0.816	0.805	0.646	0.612	0.806	0.786	0.782
Fe <sup>2+</sup>	0.089	0.103	0.073	0.177	0.142	0.167	0.131	0.129	0.055	0.061	0.125	0.194	0.199	0.120	0.053	0.057
Mn	0.003	0.003	0.004	0.004	0.005	0.007	0.000	0.000	0.004	0.003	0.004	0.000	0.003	0.005	0.004	0.002
ΣM1	0.986	0.992	0.984	0.998	0.980	0.990	1.000	1.000	0.983	0.980	1.000	1.000	1.000	0.998	0.983	0.980
Fe <sup>2+</sup>	-	-	-	-	-	-	0.025	0.012	-	-	-	0.003	-	-	-	-
Mn	-	-	-	-	-	-	0.006	0.006	-	-	-	0.004	0.003	-	-	-
Ca	0.960	0.956	0.975	0.868	0.877	0.879	0.106	0.123	0.974	0.978	0.954	0.829	0.799	0.955	0.969	0.974
Na	0.054	0.052	0.041	0.134	0.143	0.131	0.863	0.859	0.043	0.042	0.046	0.164	0.198	0.047	0.048	0.047
ΣM2	1.014	1.008	1.016	1.002	1.020	1.010	1.000	1.000	1.017	1.020	1.000	1.000	0.999	1.002	1.017	1.020
En mol %	38.87	40.66	41.53	36.20	35.68	36.26	--	--	41.84	41.44	41.25	35.87	34.78	41.38	40.54	40.34
Fs	10.87	9.92	8.81	16.92	17.13	16.35	--	--	8.73	8.89	9.88	18.08	19.85	9.61	9.46	9.41
Wo	50.26	49.41	49.66	46.88	47.19	47.39	--	--	49.43	49.66	48.87	46.05	45.37	49.01	49.99	50.25
Q	--	--	--	--	--	--	19.12	18.35	--	--	--	--	--	--	--	--
Jd	--	--	--	--	--	--	3.98	3.87	--	--	--	--	--	--	--	--
Ae	--	--	--	--	--	--	76.90	77.78	--	--	--	--	--	--	--	--
Mg#	78.40	80.63	82.83	68.45	67.89	69.40	15.95	18.54	83.06	82.61	81.03	66.75	64.02	81.54	81.40	81.23
Q	1.79	1.85	1.86	1.72	1.68	1.72	0.40	0.42	1.85	1.86	1.88	1.67	1.61	1.88	1.81	1.81
J	0.11	0.10	0.08	0.27	0.29	0.26	1.73	1.72	0.09	0.08	0.09	0.33	0.40	0.09	0.10	0.09

The number of ions is based on 4 cations and 6 atoms of oxygen per formula unit.

and aegirine-rich aegirine-augite (Fig. 5). The magnesium number (Mg#) varies from 84.7 to 16.1. Figures 6, 7 and 8 show four populations centered around Mg# values of 80, 70, 55 and 20. These groups define a differentiation trend with enrichment in Na and Fe<sup>3+</sup>, and concave-upward profiles in each evolving segment. This characteristic trend suggests the existence of indepen-

dent differentiation within each group. In the case of the pyroxene from dyke 3, the compositions are distributed in three groups separated by compositional gaps, showing evidence of extensive differentiation.

In the Mg#–Ca diagram (Fig. 6), the pyroxene compositions in each group define a curved trajectory of decreasing Ca with declining Mg#. A compositional gap

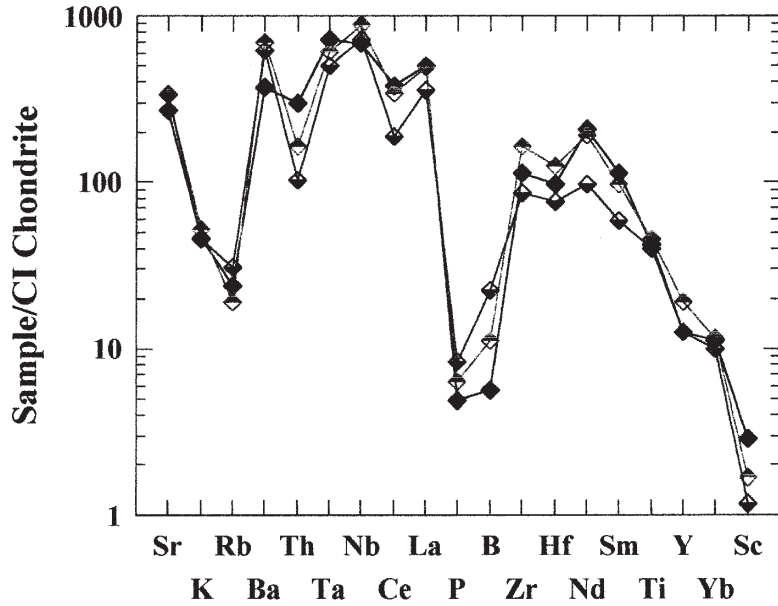


FIG. 4. Chondrite-normalized diagram (normalization values of McDonough & Sun 1995) for the melanephelinite host-rock (filled rhomb), ijolitic pegmatite (rhomb with upper half filled) and zeolite-bearing ijolitic pegmatite (rhomb with lower half filled) at La Madera.

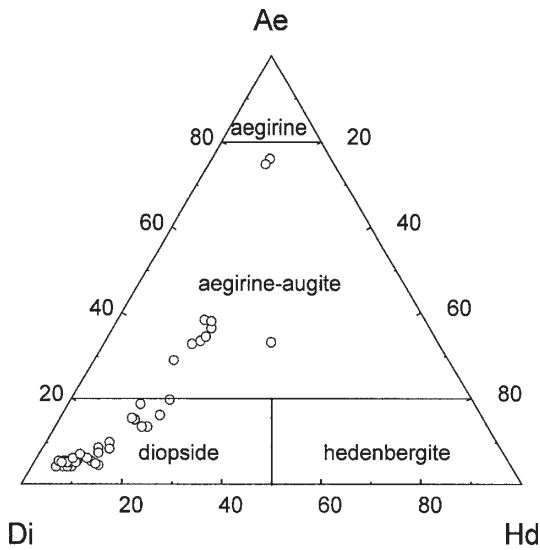


FIG. 5. Diopside (Di)–aegirine (Ae)–hedenbergite (Hd) triangular diagram showing pyroxene compositions from the ijolitic pegmatites, classified according to IMA recommendations (Morimoto 1988).

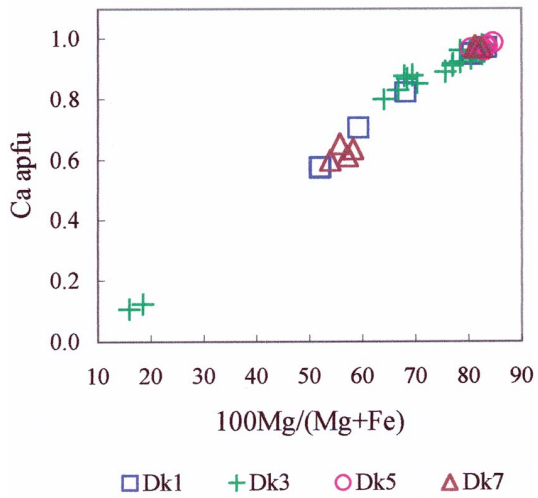


FIG. 6. Variation diagram showing the compositions of pyroxene from the La Madera ijolitic pegmatites in terms of Mg# = 100 Mg/(Mg + Fe) versus Ca in apfu.

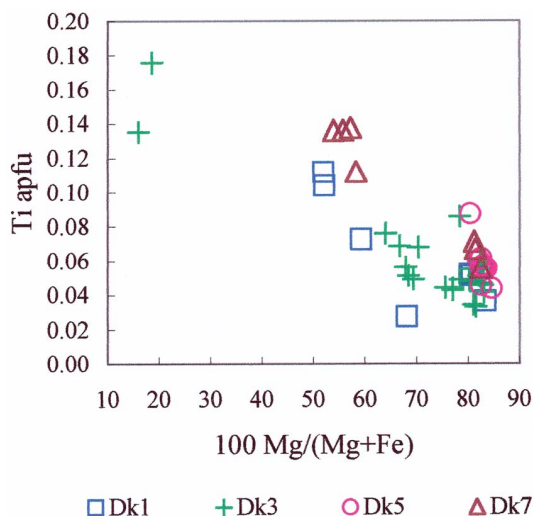


FIG. 7. Variation diagram showing the compositions of pyroxene from the La Madera ijolitic pegmatites in terms of  $Mg\# = 100 \text{ Mg}/(\text{Mg} + \text{Fe})$  versus Ti in apfu.

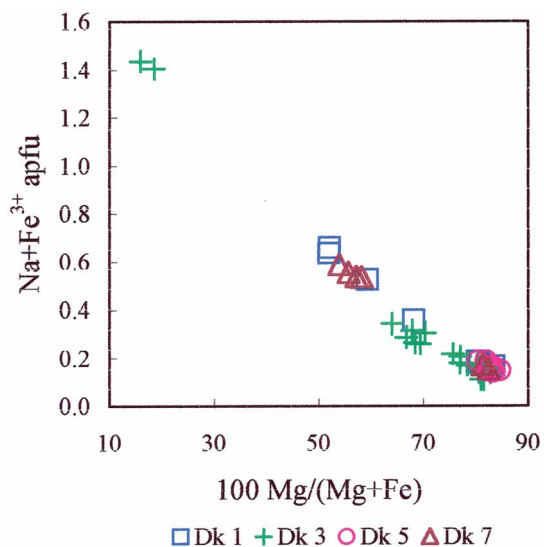


FIG. 8. Variation diagram showing the compositions of pyroxene from the La Madera ijolitic pegmatites in terms of  $Mg\# = 100 \text{ Mg}/(\text{Mg} + \text{Fe})$  versus  $\text{Na} + \text{Fe}^{3+}$  in apfu.

is particularly evident in pyroxene of dyke 3. An overall trend of increasing Ti or  $\text{Na} + \text{Fe}^{3+}$  content with fractionation is shown in the  $Mg\# - \text{Ti}$  and  $Mg\# - \text{Na} + \text{Fe}^{3+}$  diagrams (Figs. 7, 8). Nevertheless, this increase does not define a single trajectory, but within each group

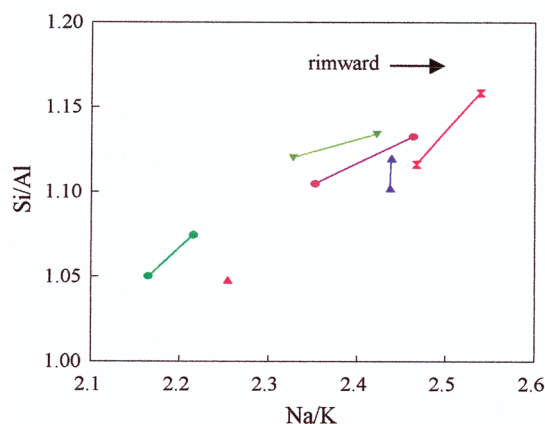


FIG. 9. Variation diagram showing the compositional zoning of nepheline crystals from the La Madera ijolitic pegmatites in terms of their  $\text{Si}/\text{Al}$  versus  $\text{Na}/\text{K}$  values.

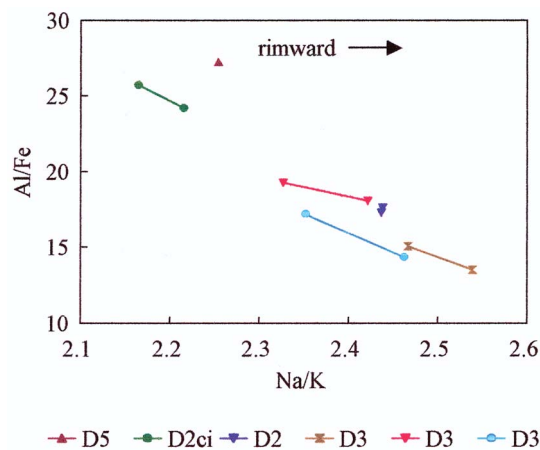


FIG. 10. Variation diagram showing the compositional zoning of nepheline crystals from the La Madera ijolitic pegmatites on the basis of their  $\text{Al}/\text{Fe}$  versus  $\text{Na}/\text{K}$  values.

of similar  $Mg\#$ , there are slightly separated trends for the pyroxenes of each dyke, and almost always there is a compositional gap between them. Zoning profiles across pyroxene crystals show increasing Na and Ti contents with declining  $Mg\#$ .

#### Nepheline

Nepheline crystals are euhedral and display {100} and {001} crystallographic forms. They average 0.5 to 1 cm in length, but some crystals are as long as 2 cm. Table 3 presents the results of electron-microprobe

TABLE 3. REPRESENTATIVE COMPOSITIONS OF NEPHELINE IN PEGMATITIC IJOLITE, LA MADERA SUITE, ARGENTINA

Sample	MP5113	MP261	MP261	MP262	MP262	MP331	MP331	MP332	MP332	MP333	MP333
Analysis	1	1 cr	2 1	1	2	1	2	1	2	1	2
SiO <sub>2</sub> wt.%	41.57	41.45	42.02	41.92	42.50	42.57	42.06	42.46	42.68	42.01	42.17
Al <sub>2</sub> O <sub>3</sub>	33.70	33.52	33.23	32.30	32.24	31.21	32.00	32.20	31.97	32.29	31.63
Fe <sub>2</sub> O <sub>3</sub>	1.94	2.04	2.15	2.92	2.86	3.62	3.33	2.62	2.77	2.94	3.45
CaO	0.03	0.04	0.06	0.07	0.05	0.09	0.03	0.03	0.03	0.09	0.05
Na <sub>2</sub> O	13.95	13.85	13.80	14.18	14.29	14.13	14.34	14.31	14.03	13.91	14.17
K <sub>2</sub> O	9.41	9.72	9.46	8.84	8.90	8.46	8.84	9.35	8.80	8.99	8.75
Total	100.59	100.61	100.71	100.23	100.84	100.07	100.59	100.97	100.29	100.23	100.23
Si <i>apfu</i>	8.090	8.082	8.166	8.194	8.253	8.328	8.206	8.252	8.315	8.210	8.253
Al	7.720	7.695	7.602	7.434	7.369	7.187	7.351	7.366	7.333	7.430	7.288
Fe <sup>3+</sup>	0.283	0.299	0.314	0.430	0.418	0.533	0.488	0.383	0.406	0.431	0.508
ΣT	16.092	16.076	16.081	16.058	16.040	16.048	16.045	16.001	16.054	16.071	16.048
Ca	0.006	0.007	0.012	0.014	0.010	0.018	0.007	0.007	0.007	0.020	0.010
Na	5.263	5.234	5.197	5.374	5.378	5.359	5.424	5.392	5.299	5.272	5.376
K	2.335	2.418	2.346	2.205	2.206	2.111	2.199	2.317	2.188	2.241	2.183
R	7.609	7.667	7.566	7.608	7.603	7.505	7.637	7.723	7.501	7.553	7.579
Compositions in term of end-members (mol.%)											
Ne	65.19	64.5	64.46	66.34	66.19	66.24	66.78	65.75	65.55	65.25	66.27
Ks	32.31	33.12	32.14	30.27	30.07	29.07	30.15	31.33	30.08	30.86	29.99
An	0.14	0.19	0.28	0.34	0.25	0.45	0.14	0.14	0.14	0.45	0.23
Qtz	2.45	2.17	3.11	3.04	3.48	4.24	2.93	2.77	4.22	3.43	3.52

References: R = Na + K + 2Ca; total iron expressed as Fe<sub>2</sub>O<sub>3</sub>; 1st digit: dyke number, 2nd digit: thin section number, 3rd digit: point of analysis, c: core, i: intermediate zone, r: rim). The number of ions, expressed in atoms per formula unit (*apfu*), is based on 32 atoms of oxygen.

analyses. The sum of Si + Al + Fe in tetrahedral sites should be 16 based of 32 atoms of oxygen, but is invariably slightly higher and variable, with an average of 16.056. The crystals are optically homogeneous but are chemically zoned, even though the K + Na content is approximately constant (7.51 *apfu*), the Si/Al – Na/K correlation (Fig. 9) shows that the degree of replacement of K for Na and of Al for Si is greater in the core than in the rim. The Al/Fe *versus* Na/K variation (Fig. 10) shows that the replacement of Al by Fe increases toward the rim. The values of Ne, Ks and Qtz are projected in the nepheline – kalsilite – quartz phase diagram (Fig. 11) according to the procedure by Kononova *et al.* (1967). The isotherms were determined by Hamilton (1961). The nepheline from the La Madera ijolitic pegmatites are richer in K and Si than most examples of nepheline in ijolites, melteigites and nepheline syenites, which plot at lower temperatures.

#### Analcime

Analcime is sporadically present in the pegmatites, preferentially occurring at the top of the subhorizontal dykes of ijolitic pegmatites, though it is more commonly

found in segregation vesicles; in both type of occurrences, it is idiomorphic, very light green and displays the {112} crystallographic form as crystals 1 cm across that are invariably included in glass or in the devitrified groundmass. Analcime almost never maintains its identity because it is replaced by phillipsite-Na. Its previous existence is recognized owing to the pseudomorphic state of the replacing phillipsite-Na, which preserves a similar chemical composition, but is slightly more hydrated than analcime.

#### Phillipsite-Na

Phillipsite-Na, the most abundant zeolite, is present in several occurrences. In the melanephelinite, it usually forms the central portions of segregation vesicles. Where present in the small, irregular dykelets, it rims the pyroxene and apatite crystals. More commonly, phillipsite-Na fills amygdules in the ijolitic pegmatite dykes, almost in all cases included in the groundmass. The amygdules have a centripetal growth of phillipsite-Na, and they are either completely filled or contain druses of crystals coated by chlorite or iron oxides. In some occurrences, calcite or a cubic zeolite is present

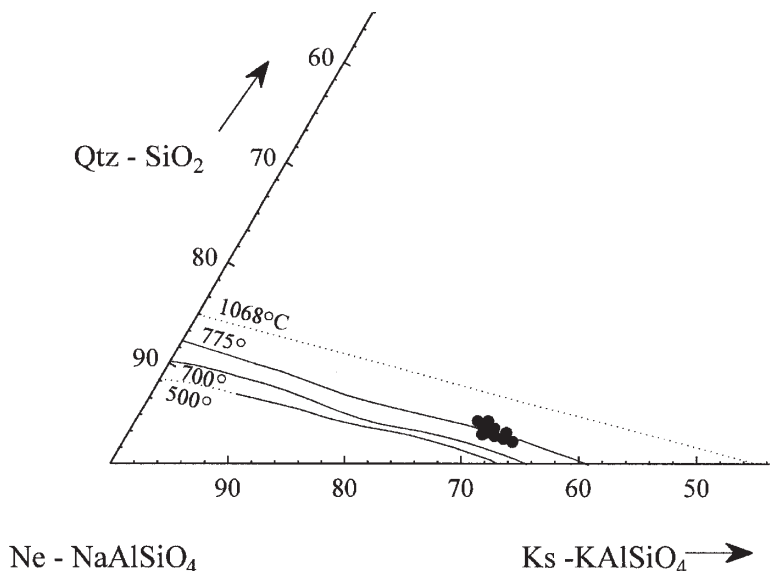


FIG. 11. Nepheline compositions from the La Madera ijolitic pegmatites plotted in the nepheline (Ne) – kalsilite (Ks) – quartz (Qtz) triangular diagram. Isotherms after Hamilton (1961).

TABLE 4. REPRESENTATIVE COMPOSITIONS OF PHILLIPSITE-Na IN PEGMATITIC IJOLITE, LA MADERA SUITE, ARGENTINA

Sample	MP 341	MP 341	MP 342	MP 344	MP 345	MP 262	MP 262	MP 262	MP 263	MP X16.1	MP X16.2	MP X16.2
Analysis	1	2	3	5	6	9	10	11	12	13	14	15
SiO <sub>2</sub> wt.%	52.46	52.27	51.54	52.17	53.56	52.54	51.22	52.99	52.09	52.26	52.51	52.48
Al <sub>2</sub> O <sub>3</sub>	27.80	28.27	28.62	28.43	28.60	28.71	26.90	28.57	28.46	28.37	28.11	28.38
CaO	0.06	0.07	0.05	0.00	0.06	0.04	0.14	0.07	0.04	0.11	0.10	0.10
BaO	0.01	0.03	0.00	0.00	0.00	0.02	0.11	0.02	0.00	0.00	0.01	0.01
Na <sub>2</sub> O	9.31	9.55	9.32	8.74	7.96	8.29	8.29	8.05	8.15	9.90	9.59	9.59
K <sub>2</sub> O	0.08	0.07	0.01	0.03	0.04	0.06	0.36	0.05	0.03	0.15	0.10	0.10
H <sub>2</sub> O	8.00	8.00	8.00	8.00	8.00	8.00	8.00	8.00	8.00	8.00	8.00	8.00
H <sub>2</sub> O <sup>+</sup>	3.00	3.00	3.00	3.00	3.00	3.00	3.00	3.00	3.00	3.00	3.00	3.00
Total	100.72	101.26	100.54	100.37	101.22	100.66	98.02	100.75	99.77	101.79	101.42	101.66
Si <i>apfu</i>	10.286	10.205	10.133	10.236	10.357	10.254	10.344	10.310	10.261	10.167	10.213	10.203
Al	6.424	6.504	6.631	6.574	6.518	6.604	6.402	6.554	6.607	6.504	6.443	6.502
Ca	0.010	0.014	0.010	0.000	0.012	0.008	0.030	0.014	0.008	0.023	0.050	0.021
Ba	0.000	0.002	0.000	0.000	0.000	0.002	0.009	0.001	0.000	0.000	0.003	0.001
Na	3.540	3.615	3.553	3.325	2.984	3.137	3.246	3.038	3.113	3.735	3.688	3.615
K	0.020	0.017	0.002	0.007	0.010	0.015	0.093	0.012	0.007	0.037	0.025	0.025
H <sub>2</sub> O	7.772	7.689	7.743	7.727	7.616	7.686	7.954	7.666	7.758	7.662	7.660	7.656

References: M: Madera, P: pegmatite, 1st digit: dyke number, 2nd digit: thin-section number, 3rd digit: point of analysis. The number of ions, expressed in atoms per formula unit (*apfu*), is based on 32 atoms of oxygen.

toward the core of the amygdule. In other occurrences, the amygdules are squeezed between pyroxene crystals, nepheline and mesostasis, developing invaginations, in

some cases almost strangled, or closed up by brown mesostasis. In other dykes, the phillipsite-Na replaces analcime and nepheline, with pyroxene relics.

TABLE 5. REPRESENTATIVE COMPOSITIONS OF GROUNDMASS IN PEGMATITIC IJOLITE, LA MADERA SUITE, ARGENTINA

Sample	MP341 3	MP342 4	MP343 6	MP343 7	MP344 9	MP344 10	MP344MP3434 11	MP346 12	MP347 13	MP348 15	MP349 E16
SiO <sub>2</sub> wt.%	45.58	44.26	42.20	42.39	40.46	43.59	40.21	43.12	40.22	36.61	45.67
TiO <sub>2</sub>	1.42	1.31	1.17	1.13	1.29	1.41	1.29	1.02	2.24	1.11	1.46
Al <sub>2</sub> O <sub>3</sub>	11.21	10.47	10.57	10.68	10.30	11.13	10.42	9.94	9.23	8.68	9.89
MgO	5.74	4.96	4.95	4.91	5.44	5.92	5.42	5.67	5.02	4.68	7.57
FeO	15.15	14.21	11.76	10.55	12.05	13.31	12.19	14.04	12.76	11.88	22.08
MnO	0.07	0.08	0.06	0.02	0.08	0.06	0.04	0.11	0.73	0.10	0.13
CaO	0.48	0.52	0.80	0.96	2.05	0.70	2.09	0.55	0.63	0.61	0.43
Na <sub>2</sub> O	0.23	0.29	0.16	0.13	0.23	0.24	0.17	0.26	0.26	0.18	0.29
K <sub>2</sub> O	6.46	5.95	5.21	5.03	5.25	5.90	5.30	5.96	5.78	4.84	7.14
P <sub>2</sub> O <sub>5</sub>	0.10	0.04	0.02	0.00	1.13	0.10	1.02	0.05	0.03	0.00	0.07
F	0.08	0.10	0.12	0.09	0.21	0.18	0.13	0.06	0.12	0.03	0.18
Cl	0.02	0.03	0.04	0.05	0.02	0.00	0.07	0.05	0.06	0.13	0.02
Total	86.54	82.22	77.06	75.94	78.51	82.54	78.35	80.83	77.08	68.85	94.93

Sample	MP349 E17	MP349 E18	MP349 E19	MP751 20	MP752 21	MP753 22	MP754 23	MP756 24	MP757 25	MP758 26	MP759 27
SiO <sub>2</sub> wt.%	47.51	44.31	44.36	48.73	50.15	47.69	47.07	47.19	47.14	47.59	49.48
TiO <sub>2</sub>	1.62	1.27	1.33	1.25	1.39	1.31	1.50	1.28	1.50	1.58	1.73
Al <sub>2</sub> O <sub>3</sub>	10.65	11.51	11.10	12.75	11.91	12.16	12.42	12.8	12.24	11.22	11.04
MgO	7.54	7.07	6.62	3.94	4.17	3.96	5.14	5.69	4.86	4.42	4.74
FeO	18.08	14.24	15.06	12.49	14.23	13.30	13.87	13.55	14.51	12.86	14.23
MnO	0.11	0.05	0.09	0.17	0.07	0.00	0.03	0.09	0.00	0.01	0.04
CaO	0.51	0.48	0.54	1.26	1.25	1.22	1.23	1.24	1.18	1.14	1.09
Na <sub>2</sub> O	0.27	0.22	0.21	0.30	0.25	0.24	0.31	0.30	0.32	0.22	0.18
K <sub>2</sub> O	7.08	6.50	6.62	3.87	4.45	4.02	3.85	3.67	4.11	4.05	4.23
P <sub>2</sub> O <sub>5</sub>	0.11	0.05	0.06	0.05	0.00	0.00	0.04	0.01	0.03	0.01	0.00
F	0.13	0.09	0.09	0.11	0.08	0.08	0.13	0.12	0.12	0.12	0.09
Cl	0.00	0.02	0.00	0.02	0.02	0.00	0.00	0.00	0.00	0.03	0.02
Total	93.61	85.81	86.08	84.94	87.97	83.98	85.59	85.94	86.01	83.25	86.87

References: M: Madera, P: pegmatite, 1<sup>st</sup> digit: dyke number, 2<sup>nd</sup> digit: thin section number, 3<sup>rd</sup> digit: point of analysis.

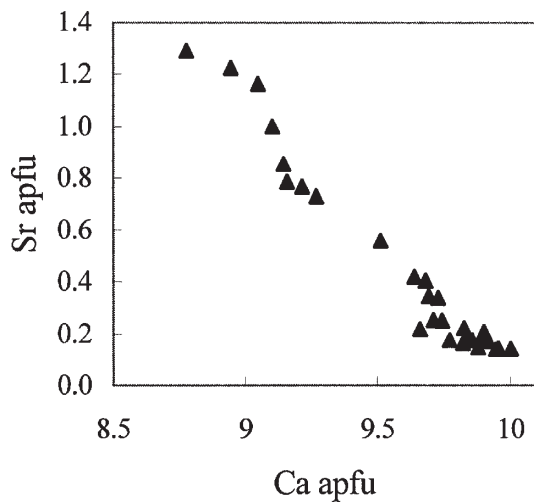


FIG. 12. Variation diagram of Sr versus Ca (*apfu*) in apatite from the La Madera ijolitic pegmatites.

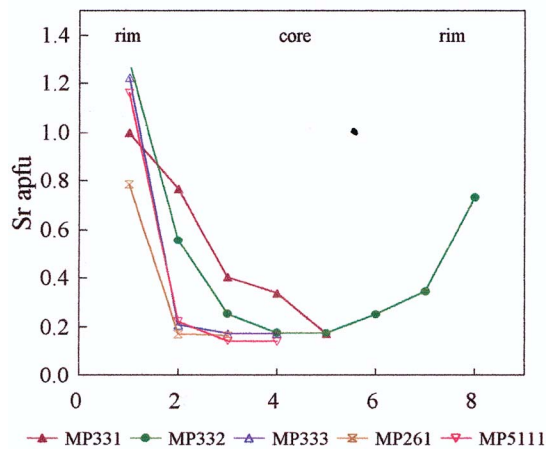


FIG. 13. Zonation in Sr (*apfu*) in apatite from the La Madera ijolitic pegmatites. References: M: Madera, P: pegmatite, 1<sup>st</sup> digit: dyke number, 2<sup>nd</sup> digit: thin section number, 3<sup>rd</sup> digit: point of analysis.

Compared to phillipsite compositions in the literature, the phillipsite-Na (Table 4) is richer in Si, Al and Na, and essentially lacks Ca, Ba and K.

*Groundmass*

The term groundmass is given to interstitial material of dirty green to reddish brown color, gritty aspect and

low degree of crystallinity. It is slightly anisotropic and has contraction-induced conchoidal fractures. In dykes, it generally occupies the central portions and is devitrified, but in the segregation vesicles, it maintains the optical and physical properties of glass. It normally contains numerous inclusions of replaced analcime, zeolite amygdules, perovskite, magnetite, apatite, amphibole and biotite. The composition of this groundmass in the pegmatites shows slight variations (Table 5). Some sec-

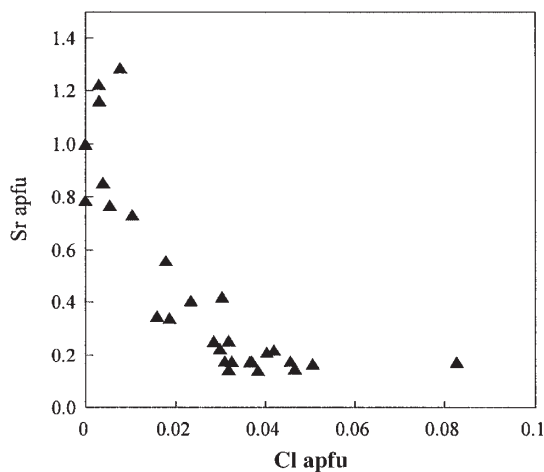


FIG. 14. Sr:Cl ratios (*apfu*) in apatite from the La Madera ijolitic pegmatites.

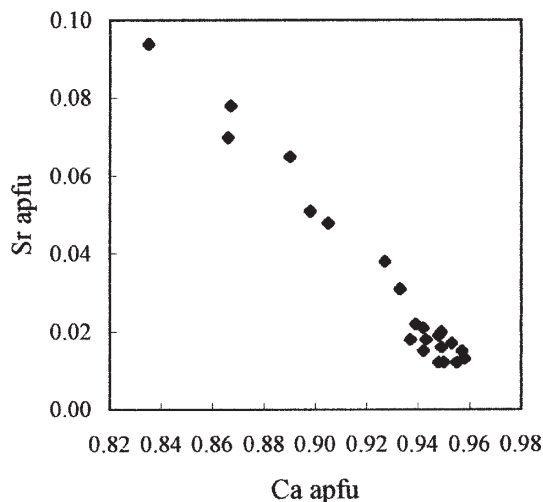


FIG. 16. Inverse Sr *versus* Ca relationship in perovskite from the La Madera ijolitic pegmatites.

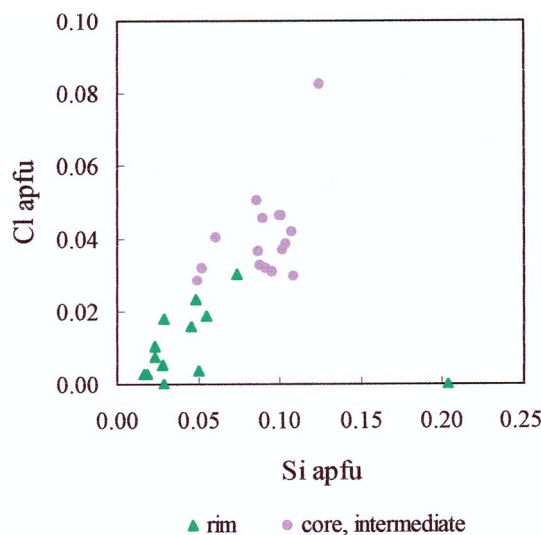


FIG. 15. There is a direct correlation between Cl and Si (*apfu*) in the zoned crystals of apatite from the La Madera ijolitic pegmatites.

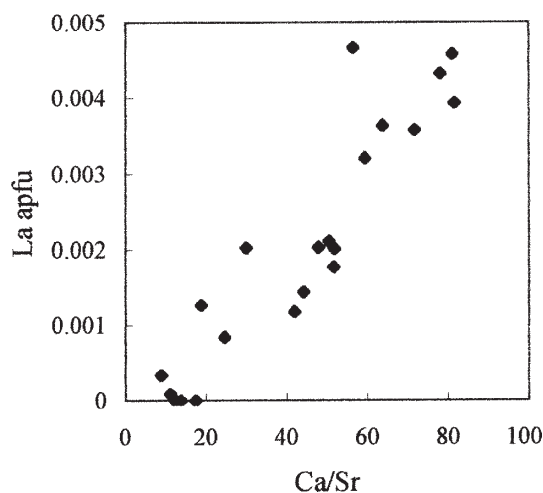


FIG. 17. Variation diagram of La *apfu* *versus* Ca/Sr in the La Madera ijolitic pegmatites.

tors show growth of an unidentified isotropic mineral that has a star-shaped habit. Its chemical composition (labeled as E in Table 5) is different from that of the mesostasis and the other analyzed minerals.

### Apatite

Apatite is a very abundant idiomorphic accessory mineral; it occurs in mm-sized crystals of long prismatic habit, typical of rapidly cooled basic rocks and is generally included in clinopyroxene, nepheline and groundmass. In this last case, it may form skeletal, hollow crystals. The crystals have a homogeneous extinction, but the chemical analyses reveal strong compositional zoning. Table 6 shows its most notable characteristic: high Sr contents, on average, 4.3% SrO. In the rims of some crystals, Sr reaches 12.44% SrO. Figure 12 shows that Sr replaces Ca, with a distribution in the zoned crystals characterized by cores with an average of 0.17 Sr<sup>2+</sup>

*apfu* that sharply increases to 1.3 Sr<sup>2+</sup> *apfu* in the rims (Fig. 13). Considering that Na contents are very low, the replacement would be <sup>71</sup>Ca<sup>2+</sup> ↔ <sup>71</sup>Sr<sup>2+</sup> toward the strontium-apatite end-member of the solid solution (Chakhmouradian *et al.* 2002). Figure 14 shows that the relation between Sr and Cl is inverse, with Cl concentrated in the cores. It seems that this distribution favors the parallel replacement of P by Si, which is more developed in the cores, as shown in Figure 15. The contents over 0.5 *apfu* of F correspond to strontian fluorapatite (Table 6); the F/Cl ratio increases, although not linearly, from the core to the rim of the crystals.

### Perovskite

Perovskite is found in pseudocubic idiomorphic crystals generally included in the groundmass. The analytical results for the major oxides are presented in Table 7. Lanthanum is present in most of the analyzed

TABLE 6. REPRESENTATIVE COMPOSITIONS OF APATITE IN PEGMATITIC IJOLITE, LA MADERA SUITE, ARGENTINA

Sample	MP 331	MP 331	MP 331	MP 331	MP 331	MP 332							
Analysis	4or	8ir	9ir	10i	11c	12or	13io	14ii	15c	16c	17ii	18io	19ir
P <sub>2</sub> O <sub>5</sub> , wt. %	39.79	40.63	40.70	41.01	41.02	39.17	40.44	41.40	40.84	41.18	41.29	41.03	40.34
SiO <sub>2</sub>	0.16	0.16	0.28	0.32	0.60	0.13	0.17	0.30	0.55	0.53	0.29	0.27	0.13
La <sub>2</sub> O <sub>3</sub>	0.12	0.00	0.06	0.05	0.08	0.10	0.00	0.05	0.14	0.11	0.07	0.00	0.00
Ce <sub>2</sub> O <sub>3</sub>	0.00	0.01	0.00	0.07	0.13	0.07	0.02	0.05	0.10	0.09	0.07	0.07	0.02
CaO	48.04	49.40	52.59	53.01	53.80	45.82	51.38	53.27	53.74	53.48	53.41	52.84	49.60
MnO	0.02	0.01	0.03	0.00	0.00	0.05	0.00	0.00	0.00	0.00	0.00	0.03	0.03
FeO <sup>t</sup>	0.18	0.07	0.02	0.00	0.00	0.05	0.03	0.05	0.08	0.13	0.04	0.02	0.01
SrO	9.76	7.60	4.06	3.42	1.78	12.44	5.58	2.59	1.79	1.79	2.56	3.48	7.22
Na <sub>2</sub> O	0.10	0.10	0.13	0.12	0.09	0.07	0.11	0.11	0.13	0.16	0.10	0.10	0.12
F	3.17	3.48	3.56	3.37	3.37	3.61	3.83	3.60	3.33	3.40	3.62	3.54	3.72
Cl	0.00	0.02	0.08	0.06	0.13	0.03	0.06	0.11	0.11	0.16	0.10	0.05	0.04
Sum	101.34	101.47	101.52	101.43	100.99	101.53	101.63	101.52	100.83	101.02	101.55	101.44	101.22
-O=F	1.34	1.47	1.50	1.42	1.42	1.52	1.61	1.52	1.40	1.43	1.52	1.49	1.57
-O=Cl	0.00	0.00	0.02	0.01	0.03	0.01	0.01	0.02	0.02	0.04	0.02	0.01	0.01
Total	100.00	100.00	100.00	100.00	99.54	100.00	100.00	99.98	99.40	99.56	100.00	99.93	99.65
P <i>apfu</i>	5.957	5.989	5.921	5.947	5.928	5.929	5.916	5.964	5.920	5.946	5.953	5.949	5.958
Si	0.029	0.028	0.049	0.055	0.102	0.023	0.029	0.052	0.095	0.090	0.049	0.046	0.023
La	0.008	0.000	0.004	0.003	0.005	0.006	0.000	0.003	0.009	0.007	0.004	0.000	0.000
Ce	0.000	0.001	0.000	0.004	0.008	0.004	0.001	0.003	0.006	0.006	0.004	0.004	0.001
Ca	9.104	9.216	9.683	9.729	9.839	8.777	9.512	9.712	9.857	9.773	9.744	9.695	9.270
Mn	0.002	0.001	0.004	0.000	0.000	0.008	0.000	0.000	0.000	0.000	0.000	0.004	0.005
Fe <sup>2+</sup>	0.026	0.010	0.003	0.000	0.000	0.007	0.004	0.007	0.012	0.018	0.006	0.004	0.002
Sr	1.001	0.767	0.405	0.339	0.176	1.289	0.559	0.255	0.178	0.177	0.253	0.346	0.731
Na	0.034	0.033	0.044	0.040	0.029	0.023	0.038	0.036	0.044	0.052	0.034	0.034	0.039
F	1.775	1.917	1.933	1.827	1.819	2.042	2.092	1.936	1.805	1.836	1.949	1.916	2.052
Cl	0.000	0.005	0.023	0.019	0.037	0.008	0.018	0.032	0.031	0.046	0.029	0.016	0.010
Total	17.936	17.967	18.068	17.963	17.943	18.116	18.170	18.001	17.957	17.951	18.024	18.012	18.091

References: M: Madera, P: pegmatite, 1<sup>st</sup> digit: dyke number, 2<sup>nd</sup> digit: thin section number, 3<sup>rd</sup> digit: point of analysis, c: core, i: intermediate zone, r: rim. The number of ions, expressed in atoms per formula unit (*apfu*), is based on 26 atoms of (O,F,Cl).

samples; it is not the most abundant rare-earth element (REE), qualitative energy-dispersion spectra demonstrated the presence of the middle REE as well. The latter possibly represent an additional 1 or 2 wt.%, which would bring the analytical total in each case close to 100%. Strontium values are high (Sr replaces Ca, as is evident in the Ca versus Sr diagram, Fig. 16), and increases from the core to the rim. The La versus Ca/Sr diagram (Fig. 17) shows that La is concentrated in the core and diminishes toward the rim of the crystals, the opposite behavior of Sr. The Nb/Ti versus Ca/Sr diagram (Fig. 18) shows that during differentiation, concomitant with the replacement of Ca by Sr, a replacement of Ti by Nb occurred, with the charge differences compensated by the coupled substitution of Na by Ca, as indicated by Deer *et al.* (1962).

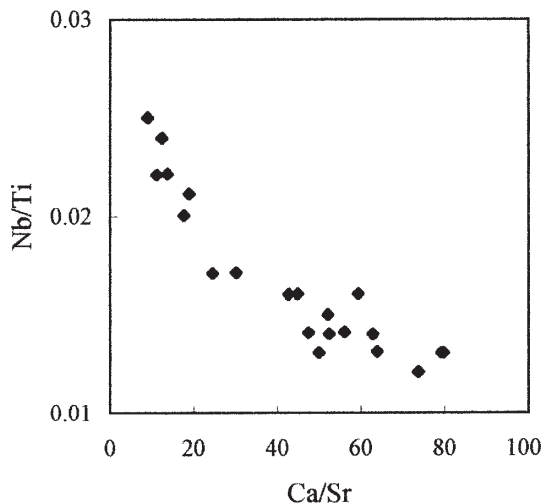


Fig. 18. Nb/Ti versus Ca/Sr plot for perovskite from the La Madera ijolitic pegmatites.

*Magnetite*

Magnetite is the most abundant opaque mineral in the ijolitic pegmatites and occurs as large  $\leq 0.5$  cm octahedra with aspects of skeletal habit, which indicates

TABLE 7. REPRESENTATIVE COMPOSITIONS OF PEROVSKITE IN PEGMATITIC IJOLITE, LA MADERA SUITE, ARGENTINA

Sample	MP 121c	MP 121r	MP 121r	MP 121i	MP 122c	MP 122i	MP 122i	MP 122r	MP 122r	MP 122r	MP 122r	MP 331c	MP 331i
Analysis	1	2	3	4	6	7	8	9	10	11	11	13	14
SiO <sub>2</sub> wt.%	0.02	0.01	0.00	0.02	0.02	0.01	0.00	0.02	0.02	0.00	0.02	0.02	0.05
TiO <sub>2</sub>	56.80	56.28	56.45	56.66	57.16	56.90	56.41	57.04	56.75	55.86	56.29	56.19	
Al <sub>2</sub> O <sub>3</sub>	0.04	0.00	0.01	0.02	0.04	0.08	0.04	0.01	0.03	0.03	0.04	0.04	
Nb <sub>2</sub> O <sub>5</sub>	1.11	1.75	1.41	1.36	1.16	1.22	1.15	1.33	1.65	1.92	1.10	1.16	
La <sub>2</sub> O <sub>3</sub>	0.25	0.15	0.10	0.17	0.24	0.21	0.24	0.14	0.00	0.00	1.47	0.55	
CaO	37.96	35.97	36.91	37.58	37.92	37.46	37.81	37.67	35.88	33.98	38.09	37.86	
MnO	0.01	0.03	0.00	0.01	0.04	0.05	0.02	0.00	0.06	0.00	0.00	0.00	0.00
FeO	0.00	0.00	0.00	0.01	0.00	0.00	0.03	0.00	0.00	0.03	0.03	0.00	0.00
SrO	1.39	3.54	2.77	1.57	1.35	1.34	1.46	1.66	3.80	5.09	1.10	1.24	
Na <sub>2</sub> O	0.71	1.05	0.79	0.67	0.73	0.74	0.78	0.72	1.01	1.19	0.67	0.59	
Total	98.29	98.78	98.44	98.07	98.66	98.01	97.94	98.59	99.20	98.10	98.81	97.68	
Si <i>apfu</i>	0.001	0.000	0.000	0.001	0.001	0.000	0.000	0.000	0.001	0.000	0.000	0.001	0.001
Al	0.001	0.000	0.000	0.001	0.001	0.002	0.001	0.000	0.001	0.001	0.001	0.001	0.001
Ti	0.996	0.994	0.995	0.996	0.998	0.999	0.994	0.998	0.997	1.000	0.992	0.992	
Nb	0.013	0.021	0.017	0.016	0.014	0.015	0.014	0.016	0.020	0.024	0.013	0.014	
Fe	0.000	0.000	0.000	0.000	0.000	0.000	0.001	0.000	0.000	0.001	0.001	0.000	0.000
Mn	0.000	0.001	0.000	0.000	0.001	0.001	0.000	0.000	0.001	0.000	0.000	0.000	0.000
Na	0.032	0.048	0.036	0.031	0.033	0.034	0.036	0.032	0.046	0.055	0.031	0.027	
Ca	0.948	0.905	0.927	0.942	0.943	0.937	0.949	0.939	0.898	0.866	0.957	0.953	
La	0.002	0.001	0.001	0.002	0.002	0.002	0.002	0.001	0.000	0.000	0.004	0.005	
Sr	0.019	0.048	0.038	0.021	0.018	0.018	0.020	0.022	0.051	0.070	0.015	0.017	
Total	2.012	2.018	2.014	2.010	2.011	2.008	2.017	2.008	2.015	2.017	2.014	2.010	

References: M: Madera, P: pegmatite, 1<sup>st</sup> digit: dyke number, 2<sup>nd</sup> digit: thin section number, 3<sup>rd</sup> digit: point of analysis, c: core, i: intermediate zone, r: rim. The number of ions, expressed in atoms per formula unit (*apfu*), is based on three atoms of oxygen.

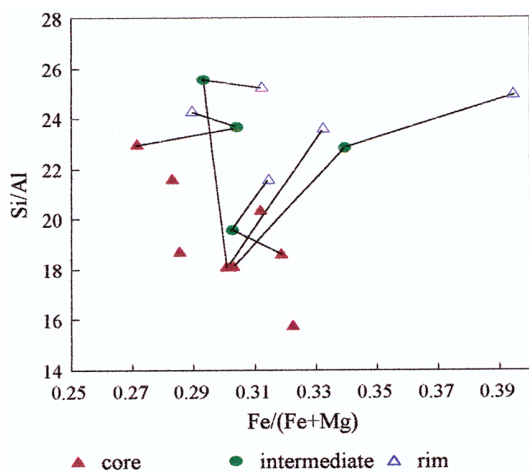


FIG. 19. Si/Al versus Fe/(Fe + Mg) (molar proportions) showing the zoning in amphibole crystals in the La Madera ijolitic pegmatites.

rapid growth. Representative compositions of magnetite (Table 8) show TiO<sub>2</sub> contents of ~20 wt.% and Mg values that reach 3.39 wt.% MgO. Manganese concentrations reach a maximum of 2.96% MnO. The magnetite of La Madera has a compositional range similar to that of the Magnet Cove alkaline complex, Arkansas (Haggerty 1976).

#### Amphiboles

Amphibole crystals are invariably found included in the groundmass as bundles of minute parallel, curved or divergent fibrous crystals. Table 9 shows representative results of chemical analyses and formulae calculated based on 23 atoms of oxygen; we adjusted the cations to 13 in the tetrahedral and octahedral sites. The estimation of the Fe<sup>3+</sup> content was done using programs by Mogessie & Tessadri (1982) and Mogessie *et al.* (1990). On the basis of the IMA classification (Leake 1978, Rock & Leake 1984, Leake *et al.* 1997), the amphiboles belong to the sodic-calcic group, and correspond to magnesiokatophorite that grade in two cases to a rim of eckermannite. In the variation diagrams (Fig. 19), the relation Si/Al, though not strongly corre-

TABLE 8. REPRESENTATIVE COMPOSITIONS OF MAGNETITE IN PEGMATITIC IJOLITE, LA MADERA SUITE, ARGENTINA

Sample	MP 121 r	MP 121 c	MP 122 r	MP 122 c	MP 123	MP 751 c	MP 751 i	MP 752 c	MP 752 i	MP 753	MP 754 c	MP 754 i	MP 755
SiO <sub>2</sub> wt.%	0.08	0.08	0.10	0.26	0.44	0.06	0.03	0.06	1.67	0.53	0.08	1.82	0.05
TiO <sub>2</sub>	19.89	19.81	20.87	19.76	19.52	20.98	20.98	21.51	21.01	22.85	21.33	22.61	20.10
Al <sub>2</sub> O <sub>3</sub>	0.59	0.51	0.34	0.56	0.53	0.34	0.36	0.32	0.73	0.29	0.26	0.69	0.53
Cr <sub>2</sub> O <sub>3</sub>	0.01	0.02	0.08	0.09	0.02	0.06	0.02	0.11	0.09	0.08	0.09	0.09	0.25
Fe <sub>2</sub> O <sub>3</sub>	28.36	28.85	26.29	28.98	28.08	28.03	27.47	25.59	22.92	21.20	26.22	19.93	28.92
MgO	3.02	2.94	2.37	2.72	2.44	2.72	2.44	1.93	1.64	1.13	1.79	1.13	3.39
MnO	0.88	0.86	1.20	0.93	1.00	0.88	0.96	0.99	1.90	2.09	1.17	2.96	0.71
FeO	42.67	42.86	44.2	43.23	42.76	44.85	45.03	46.03	43.81	46.75	46.01	45.15	42.89
Total	95.50	95.93	95.45	96.53	94.79	97.92	97.29	96.54	93.77	94.92	96.95	94.38	96.84
Si <i>apfu</i>	0.02	0.02	0.03	0.08	0.14	0.02	0.01	0.02	0.52	0.17	0.02	0.56	0.01
Al	0.22	0.18	0.12	0.20	0.19	0.12	0.13	0.12	0.27	0.11	0.10	0.25	0.19
Cr	0.00	0.00	0.02	0.02	0.00	0.01	0.00	0.03	0.02	0.02	0.02	0.02	0.06
Fe <sup>3+</sup>	6.56	6.66	6.12	6.64	6.55	6.35	6.28	5.91	5.36	4.98	6.04	4.64	6.59
Ti	4.60	4.57	4.85	4.53	4.55	4.75	4.79	4.96	4.91	5.36	4.91	5.26	4.57
Sum	11.4	11.43	11.14	11.47	11.43	11.25	11.21	11.04	11.08	10.64	11.09	10.73	11.42
Mg	1.38	1.34	1.09	1.23	1.13	1.22	1.11	0.88	0.76	0.52	0.82	0.52	1.53
Fe <sup>2+</sup>	10.97	10.99	11.43	11.01	11.09	11.29	11.43	11.81	11.39	12.20	11.78	11.68	10.86
Mn	0.23	0.22	0.31	0.24	0.26	0.23	0.25	0.26	0.50	0.55	0.30	0.78	0.18
Sum	12.58	12.55	12.83	12.48	12.48	12.74	12.79	12.95	12.65	13.27	12.90	12.98	12.57

References: M: Madera, P: pegmatite, 1st digit: dyke number, 2<sup>nd</sup> digit: thin section number, 3<sup>rd</sup> digit: point of analysis, c: core, i: intermediate zone, r: rim. The number of ions, expressed in atoms per formula unit (*apfu*), is based on 32 atoms of oxygen.

lated, tends to increase with increasing  $Fe/(Fe + Mg)$ , *i.e.*, with the degree of differentiation. Sodium is generally not affected by variations in  $Fe/(Fe + Mg)$  (Fig. 20), and thus is distinct from K, which increases significantly with the progress of fractionation (Fig. 21).

#### Other minerals

Several accessory minerals for which we still lack analytical results were noted. Biotite is a late phase found sporadically as large sheets around skeletal crystals of magnetite. Less commonly, it occupies interstices between zeolite and pyroxene. Calcite is a common late-stage mineral that generally crystallizes with phillipsite-Na in amygdules and cavities. It is considered of primary origin on the basis of its paragenesis and its  $^{13}C/^{12}C$  isotopic data. It is different texturally and isotopically from calcite in small, vertical joint-filling veins (1–2 cm width), which is interpreted to be of secondary origin.

Natrolite is present in botryoidal masses developed in cavities in sectors in which zeolites are significantly replaced. Chlorite is an occasional late-stage mineral that crystallizes in the groundmass or coats phillipsite-Na crystals in some amygdules. Hematite is present as corroded, subhedral crystals that are associated with nepheline or pyroxene and as fine secondary grains scattered in the groundmass that display red internal reflections. Goethite reaches a greater abundance as late colloform deposits in dykes with strong replacements by zeolites. A mineral found in acicular crystals was

tentatively identified as rutile. These crystals may be twinned, and are enclosed in the groundmass. Another phase is an unidentified isotropic mineral that has a star-shaped habit and is present as inclusions in the groundmass.

#### RESULTS OF OXYGEN AND CARBON ISOTOPE ANALYSES

##### Silicates and oxides

Stable isotope measurements were made on selected mineral phases from La Madera ijolite pegmatites (Table 10). Minerals chosen for analyses were previously evaluated from a well-established paragenetic sequence (see Galliski *et al.* 1992). Among selected minerals, nepheline (samples IJ02–Ne003, MMLM–Ne3) and clinopyroxene (diopside, samples IJ02–Cpx002, MMLM–Cpx3) represent the earliest stages of crystallization of the pegmatite-forming melt, whereas magnetite (sample IJ02–Mgt001) crystallized slightly later. Three generations of calcite were identified during textural analyses; the earliest occurs as the last mineral to crystallize in the hypogene association (samples IJ04–Cc005 and IJ8–Cc001), and the latest recorded (sample MMLM–Cc24) was interpreted as resulting from secondary veins.

Using the fractionation factor of Bottinga & Javoy (1973, 1975) for clinopyroxene (diopside) –  $H_2O$  at a minimum temperature of about 770°C [derived from the molar variations of the solid solution and excess  $SiO_2$  in the system Ne–Ks–Qtz (Fig. 9); see Galliski *et al.*

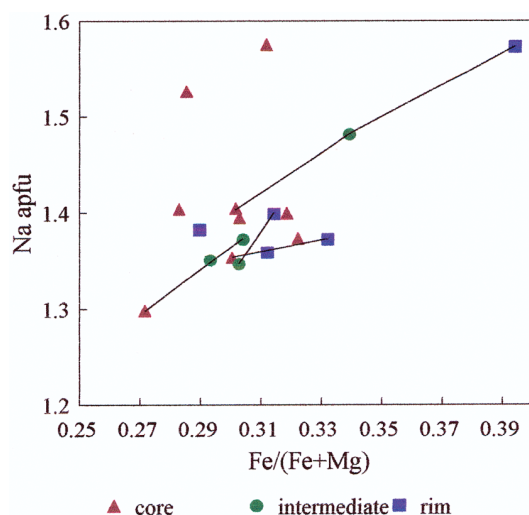


FIG. 20. Na *apfu* versus  $Fe/(Fe + Mg)$  (molar proportions) showing the zonation in amphibole crystals in the La Madera ijolitic pegmatites.

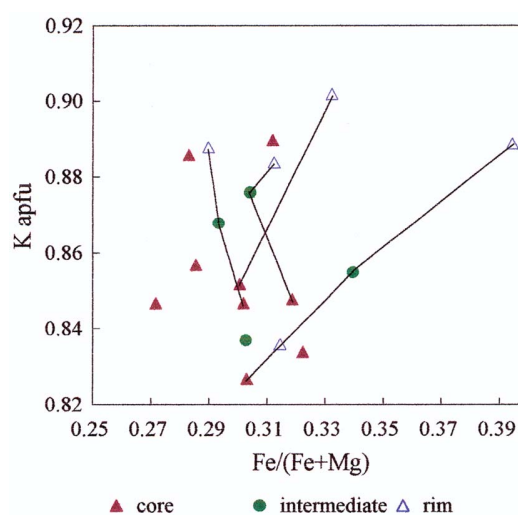


FIG. 21. Zonation in amphibole crystals from the La Madera ijolitic pegmatites, as indicated by their K (*apfu*) versus  $Fe/(Fe + Mg)$  (molar proportion).

1992], the computed values of  $\delta^{18}\text{O}_{\text{H}_2\text{O}} (770^\circ\text{C})$  for  $\text{H}_2\text{O}$  in equilibrium with diopside range from  $\sim 8.5$  (Cpx002) to  $\sim 8.2\%$  (Cpx3). Similarly, using the fractionation factor of Bottinga & Javoy (1973) for magnetite– $\text{H}_2\text{O}$  at the same temperature, the calculated  $\delta^{18}\text{O}_{\text{H}_2\text{O}} (770^\circ\text{C})$  is  $8.9\%$ . All calculated values for oxygen isotope composition of fluids in equilibrium with early paragenetic pyroxenes and magnetite suggest a magmatic origin.

### Carbonates

According to Hoefs (1987), the two main carbon reservoirs on Earth are carbonates (“heavy” C,  $\delta^{13}\text{C}_{\text{PDB}} = 0\%$ ), and reduced carbon of biological origin (“light” C,  $\delta^{13}\text{C}_{\text{PDB}} = -25\%$ ). Juvenile carbon from mantle sources shows typical  $\delta^{13}\text{C}_{\text{PDB}}$  values between  $-5$  and  $-10\%$  (Hoefs 1987). In other words, marine limestones

TABLE 9. REPRESENTATIVE COMPOSITIONS OF AMPHIBOLES IN PEGMATITIC IJOLITE, LA MADERA SUITE, ARGENTINA

Sample	MP 331c	MP 331c	MP 332c	MP 332r	MP 332i	MP 333c	MP 333i	MP 333r	MP 261c	MP 261i	MP 261r	MP 262c	MP 262i	MP 262r
Analysis	4	5	6	7	8	9	10	11	16	17	18	20	21	22
SiO <sub>2</sub> wt. %	48.15	47.91	47.94	48.04	48.78	48.24	48.89	48.96	48.29	47.97	47.84	47.33	47.36	47.76
TiO <sub>2</sub>	5.79	6.61	6.76	5.78	6.01	6.57	6.21	5.80	6.84	6.35	6.56	7.79	7.38	6.82
Al <sub>2</sub> O <sub>3</sub>	2.25	2.57	2.24	1.63	1.81	2.19	2.12	1.92	1.78	1.72	1.67	1.71	1.57	1.60
FeOt	10.78	11.54	11.01	13.96	12.29	11.54	11.06	11.49	9.83	10.92	10.19	10.78	10.69	11.21
MnO	0.14	0.18	0.10	0.18	0.18	0.20	0.17	0.12	0.12	0.19	0.18	0.19	0.16	0.16
MgO	14.00	13.62	14.22	12.03	13.42	13.85	14.30	14.06	14.80	14.02	14.02	14.08	14.45	13.85
CaO	5.10	4.72	4.58	3.71	4.19	4.79	4.82	4.32	4.95	4.89	4.90	4.80	4.66	4.48
Na <sub>2</sub> O	4.75	4.69	4.77	5.25	5.05	4.79	4.64	4.79	4.43	4.63	4.63	4.59	4.58	4.58
K <sub>2</sub> O	4.35	4.33	4.30	4.51	4.43	4.41	4.38	4.35	4.39	4.49	4.52	4.39	4.47	4.53
F	2.00	1.79	1.95	1.72	1.90	1.91	2.01	1.88	2.62	2.49	2.58	2.46	2.50	2.34
Cl	0.02	0.02	0.00	0.02	0.02	0.00	0.02	0.02	0.01	0.00	0.00	0.02	0.00	0.00
Sum	97.32	97.97	97.87	96.83	98.08	98.49	98.62	97.71	98.06	97.67	97.09	98.14	97.82	97.33
–O=F	0.84	0.75	0.82	0.73	0.80	0.81	0.85	0.79	1.10	1.05	1.09	1.03	1.05	0.99
–O=Cl	0.00	0.00	0.00	0.00	0.00	0.00	0.00	0.00	0.00	0.00	0.00	0.00	0.00	0.00
Total	96.47	97.22	97.05	96.10	97.28	97.68	97.77	96.92	96.96	96.62	96.00	97.11	96.77	96.34
Si <i>apfu</i>	7.347	7.237	7.230	7.425	7.382	7.269	7.321	7.376	7.303	7.336	7.372	7.203	7.207	7.306
<sup>IV</sup> Al	0.405	0.458	0.398	0.297	0.323	0.389	0.374	0.341	0.317	0.310	0.303	0.397	0.282	0.289
Ti	0.248	0.305	0.372	0.278	0.295	0.342	0.305	0.283	0.380	0.354	0.325	0.400	0.511	0.405
$\Sigma T$	8	8	8	8	8	8	8	8	8	8	8	8	8	8
Ti	0.423	0.454	0.403	0.401	0.396	0.410	0.401	0.381	0.406	0.384	0.443	0.501	0.342	0.388
Mg	3.184	3.066	3.196	2.771	3.026	3.110	3.191	3.157	3.335	3.195	3.220	3.193	3.277	3.158
Fe <sup>2+</sup>	1.376	1.458	1.389	1.804	1.555	1.454	1.385	1.448	1.243	1.396	1.313	1.372	1.360	1.434
Mn	0.018	0.023	0.013	0.024	0.023	0.025	0.022	0.015	0.025	0.023	0.024	0.024	0.021	0.021
$\Sigma M1, M3$	5.001	5.001	5.001	5.000	5.000	4.999	4.999	5.001	4.999	5.000	4.999	5.090	5.000	5.001
Ca	0.834	0.764	0.740	0.614	0.679	0.773	0.773	0.697	0.802	0.801	0.809	0.783	0.760	0.734
Na	1.166	1.236	1.260	1.386	1.321	1.227	1.227	1.303	1.198	1.199	1.191	1.217	1.240	1.266
$\Sigma M2$	2.000	2.000	2.000	2.000	2.000	2.000	2.000	2.000	2.000	2.000	2.000	2.000	2.000	2.000
Na	0.239	0.138	0.135	0.187	0.161	0.173	0.120	0.096	0.101	0.174	0.192	0.137	0.111	0.093
K	0.847	0.834	0.827	0.889	0.855	0.848	0.837	0.836	0.847	0.876	0.888	0.852	0.868	0.884
$\Sigma M4$	1.086	0.972	0.962	1.076	1.016	1.021	0.957	0.932	0.948	1.050	1.080	0.989	0.979	0.977

References: M: Madera, P: pegmatite, 1<sup>st</sup> digit: dyke number, 2<sup>nd</sup> digit: thin section number, 3<sup>rd</sup> digit: point of analysis, c: core, i: intermediate zone, r: rim. The number of ions, expressed in atoms per formula unit (*apfu*), is calculated on the basis of tetrahedral and octahedral (*M1*, *M2*, *M3*) sites normalized to 13 cations.

have a typical  $\delta^{13}\text{C}_{\text{PDB}} = 0\text{‰}$ , deep-seated C from  $\text{CO}_2$  in fluid inclusions, ocean-ridge basalts (MORB), carbonates and diamonds is in the range  $-5$  to  $-10\text{‰}$ , and organic C from sedimentary rocks has a  $\delta^{13}\text{C}_{\text{PDB}}$  value typically lower than  $-20\text{‰}$ . In hydrothermal carbonates, the  $\delta^{13}\text{C}$  value also depends on several variables, such as the total concentration of carbon,  $f(\text{O}_2)$ , pH, temperature, and the ionic strength of the fluid (Ohmoto 1972). Most juvenile carbonates have  $\delta^{13}\text{C}_{\text{PDB}}$  values between  $-7$  and  $-5\text{‰}$ , suggesting a deep-seated origin; however, the same values can be generated by simple mixing between carbonate-derived and organically derived  $\text{CO}_2$  ( $0\text{‰}$  to  $-25\text{‰}$ ) (Hoefs 1987). The La Madera calcite samples IJ-004 – Cc005 and IJ8 – Cc001 (early stage?) have  $\delta^{13}\text{C}_{\text{PDB}}$  values of  $-8.4$  and  $-8.1\text{‰}$ , suggesting that carbon was derived from a deep-seated source, perhaps slightly contaminated by an organic carbon source that could be C leached from meta-sedimentary country-rocks (lutite) during ascent of the melanephelinitic melt. Although mixing of  $\text{CO}_2$  derived from carbonate (marine limestones) and from an organic source could also explain values of  $\delta^{13}\text{C}_{\text{PDB}}$  between  $-8$  and  $-8.5\text{‰}$ , this cannot be the case for La Madera carbonates, for which a mantle-derived origin is supported by the rock itself. The value for calcite sample IJ-004 – Cc24 (late-stage vein),  $\delta^{13}\text{C}_{\text{PDB}} = -2.5\text{‰}$ , is enriched in the heavier isotope relative to the earlier-stage calcite (Cc005). Enrichment in  $^{13}\text{C}$  from early- to late-stage gangue carbonates in hydrothermal ore deposits (Rye & Ohmoto 1974) could result from: 1) cooling of the ore fluid, 2) decreasing  $\text{CO}_2:\text{CH}_4$  ratio in the fluid, and 3) increasing input of  $\text{CO}_2$  from other sources (Hoefs 1987). At La Madera, late-stage cross-cutting veins of calcite could have been generated from a cooling infiltrating fluid (probably mixed with meteoric water) or, less probably, from local addition of  $\text{CO}_2$  from a marble or other inorganic C-bearing metasedimentary source.

Computation of the oxygen isotopic compositions of  $\text{H}_2\text{O}$  in equilibrium with earlier Cc-005 calcite, assuming that the carbonate crystallized in the range between  $500$  and  $300^\circ\text{C}$ , yields  $\delta^{18}\text{O}_{\text{H}_2\text{O}}$  values between  $\sim 26.6$  ( $500^\circ\text{C}$ ) and  $22.8\text{‰}$  ( $300^\circ\text{C}$ ). Equivalent values for the

late calcite veins are  $\sim 21.1\text{‰}$  at an assumed temperature of  $300^\circ\text{C}$  and  $14.0\text{‰}$  at  $150^\circ\text{C}$ . Computed values of  $\text{H}_2\text{O}$  related to early and late stages of calcite precipitation are both enriched in  $^{18}\text{O}$  beyond the upper limit of magmatic  $\text{H}_2\text{O}$ , and plot within the metamorphic  $\text{H}_2\text{O}$  field. The lighter values of the late calcite vein could result from interaction of these  $^{18}\text{O}$ -rich fluids with meteoric water. Some hydrothermal fluids related to sources in the deep crust also fall into the metamorphic water field (Hoefs 1987). Values of  $\delta^{18}\text{O}$ -rich samples of calcite plot well within fields of data compiled by Taylor (1987) from quartz-carbonate gold veins ( $\pm W$ ). Taylor (1987) suggested that large volumes of basaltic magma emplaced at the base of the crust could generate  $\text{H}_2\text{O}$  owing to metamorphic dehydration, exsolution from the magma, and  $\text{CO}_2$  brought in from the mantle.

## DISCUSSION

### *Mechanism of generation of the pegmatite-forming melt*

The remarkable similarities in mineral species and the tight correspondence in chemical composition (Fig. 4) between the olivine melanephelinite and the veins of ijolitic pegmatites establish a strong parental link. Consequently, the ijolitic pegmatites could have been derived through fractional crystallization of the olivine melaphelinitic magma or could be a different pulse of magma of similar composition that was emplaced afterward. This last possibility is considered less probable owing to the following arguments: 1) the melanephelinite is a volcanic rock. It is highly unlikely to have been affected by intrusive pulses after its cooling at such a shallow level. 2) The ijolitic pegmatites are severely depleted in Mg, less so in Fe and Ni, and especially in Sc and Cr in relation to the melanephelinite (Fig. 4). There was thus efficient removal of those elements, owing to the crystallization of olivine and pyroxene in the melanephelinitic magma.

Studies of vesicle formation and of the segregation of veins in basaltic flows shed much light on the mechanism of differentiation and migration of evolved fractions (Smith 1967, Lindsley *et al.* 1971, Anderson *et al.* 1984, McMillan *et al.* 1987, Puffer & Horter 1993), especially in the lava lakes of picritic composition in Hawai'i (Helz 1980, Helz *et al.* 1989). In these cases, where the cooling of the magma occurs from the top down and the bottom up, toward the center of the lava lake, several independent mechanisms of differentiation occur (Helz *et al.* 1989), of which the most pertinent to our context is that of the formation of segregation vesicles and segregation veins.

The crystallization and gravitational concentration of the early crystallizing phases, mainly olivine and, to a lesser degree, pyroxene and perovskite at the base of the flow, would have formed a network with inter-

TABLE 10. OXYGEN AND CARBON ISOTOPE RESULTS, MINERALS OF THE PEGMATITIC IJOLITE, LA MADERA SUITE, ARGENTINA

Mineral	Sample	$\delta^{18}\text{O}_{\text{snow}}$	$\delta^{13}\text{C}_{\text{PDB}}$
Nepheline	IJ02 – Ne003	6.6	
Nepheline	MMLM – Ne3	7.0	
Diopside	IJ02 – Cpx002	6.1	
Diopside	MMLM – Cpx3	5.8	
Magnetite	IJ02 – Mgt001	3.8	
Calcite	IJ04 – Cc005	27.8	-8.3
Calcite	IJ8 – Cc001	26.6	-8.1
Calcite	MMLM – Cc24	26.1	-2.5

The  $\delta$  values are expressed in ‰.

crystalline space connected and occupied by a melt enriched in incompatible and volatile elements. This is shown in the data of Table 1 and in the *spider* diagram (Fig. 4), where it is observed that the higher concentrations of Mg, Fe, Cr, Ni, Sc, Sm, Th, La, Ce and Nd in the olivine melaphelinite and the increase of Ba, Rb, K, Nb, P, Cs and U in the pegmatite-forming melts can be perfectly explained by the crystallization of those anhydrous phases. The consequent lower density acquired by the remaining melt and its progressive decrease in viscosity would have made the upward migration easier until the residual melts coalesced and formed a layer of low-density melt in the base of the lava pond, in its middle section (Fig. 22). Once a certain density-contrast threshold between this layer and the hottest and densest melt of the ponded middle part of the lava flow has been passed, there would then have occurred a diapiric transference of the low-density melt. This general process is supported by two textural evidences observed in outcrops: 1) the existence of restricted millimeter-sized domains dispersed across the melanephelinite characterized by the presence of zeolites + biotite, which represent spots with stronger specific differentiation gradients; these zeolite- and biotite-bearing domains are interpreted as fractions enriched in incompatible elements and H<sub>2</sub>O that remained occluded in the evolving system; 2) the “frozen image” given by the spatial distribution of the centimeter-sized segregation vesicles

scattered across the melanephelinite in the face of the quarry, resembling droplets ascending in a more dense environment.

The coalescence of the segregation vesicles beneath the interphase between the rigid, totally crystallized upper part of the lava flow and the partially molten middle sections produced a low-density layer of melt. *In situ* crystallization of this melt or its permissive emplacement in the fractures of the upper and consolidated part of the lava flow then resulted in the formation of the ijolitic pegmatite dykes.

#### *Crystallization of the pegmatites*

The crystallization process of the pegmatite-forming melt in fractures can be traced with the help of the evolving composition of the minerals, their paragenetic sequence, textural relationships and the bulk-rock composition of the ijolitic pegmatites. It is evident from the isotopic results that pyroxene and magnetite in the pegmatites crystallized from a system without significant inflow of meteoric water.

The compositional variation recorded by the pyroxene in the pegmatites, from diopside to aegirine-augite (Fig. 5), is neither linear nor continuous, and there are four groups with different Mg#. Nevertheless, the different Mg# values do not correspond to different dykes or even to different crystals, but the same crystal may

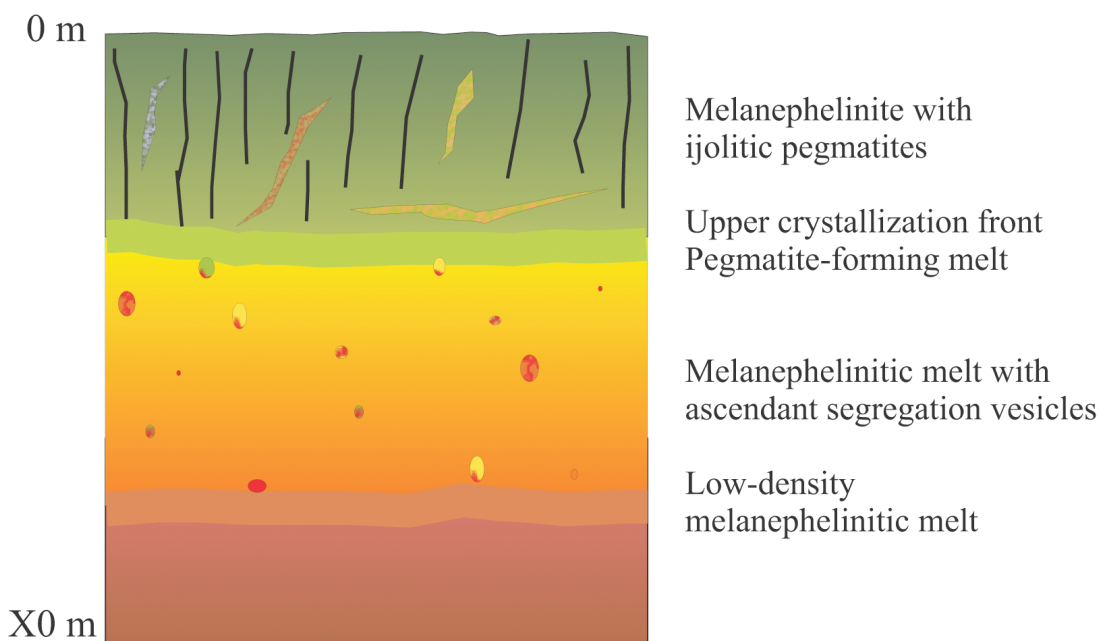


FIG. 22. Cartoon representation showing the origin of ijolitic pegmatites from La Madera, modified from Helz *et al.* (1989) and Puffer & Horter (1993).

contain compositions of two or three different groups. The zoning must be attributed to adjustments of the crystal–melt system.

The evolving compositional trend is explained because the  $aMgO$  is greater than that of the other oxides, therefore it expands crystallization in the diopside field. As the melt increased in both  $Fe^{2+}$  and  $Fe^{3+}$  and alkalinity, the crystallizing pyroxenes evolved to aegirine-augite, instead of hedenbergite, because hedenbergite was not a stable phase in these alkaline liquids (Schairer & Yoder 1962).

The zoning of nepheline in the ijolitic pegmatites manifests itself as a rimward replacement of K by Na and of Al by Si and Fe (Figs. 9, 10), suggesting that the crystals grew under conditions of disequilibrium growth at high temperatures. The nepheline compositions are unusually rich in the kalsilite component for plutonic rocks, with values close to  $(Ne_{66}Ks_{31}Qtz_3)$  compared to the Buerger–Morozewicz convergence compositions of  $Ne_{73-75}Ks_{24-27}Qtz_4$ , as defined by Tilley (1954). This enrichment in kalsilite in the La Madera nephelines is a consequence of crystallization at high temperatures, close to or higher than the minimum indicated by the 775°C curve (Fig. 11).

Analcime was not stable at low temperatures, but its prior existence can be recognized by the phillipsite-Na pseudomorphs. Its stability seems to be a function of higher  $P(H_2O)$ ; at lower  $P(H_2O)$ , nepheline is formed instead. In the segregation vesicles with abundant glass, whose solidus temperatures were depressed by the increasing  $H_2O$  content, analcime crystallized instead of nepheline, forming a fringe of trapezohedral crystals inward of the pyroxene-rich wall zone (Fig. 3H). Dykelet analcime is contained in the groundmass and preferentially in the upper portions of the dykelets, suggesting that an aqueous phase was concentrated by gravitational differentiation in the upper parts once that an adequate degree of differentiation was reached.

Perovskite is a mineral that possibly started to crystallize early in the evolution of the melanephelinitic melt, as shown in the bulk-rock negative Th anomaly. In the later stages of crystallization, as characterized by the dark ijolites, perovskite incorporated La, Ce, Sm and specially Nd, provoking the negative Nd anomaly that characterizes the zeolite-bearing ijolitic pegmatites. The remaining Ti in the melt that was not used to form perovskite was incorporated by pyroxene and magnetite in such a way that the Ti contents in the different rocks were maintained at approximately constant values. The progressive enrichment in Nb, REE and Sr in perovskite with the evolution of the dark dykelets is characteristic of perovskite from alkaline complexes, such as at Khibina, Russia (Veksler & Teptev 1990), although not to the levels required to form loparite.

Apatite crystals of the ijolitic pegmatites are strongly enriched in Sr, up to levels comparable to the apatite of the alkaline complexes of the Kola Peninsula (Deer *et al.* 1962). The crystals are strongly zoned, and the ten-

dency of enrichment in Sr with fractionation follows the differentiation patterns from ijolites to urtites as found by Le Bas & Handley (1979) in populations of apatite from ijolitic and carbonatitic rocks. The existence of acicular hollow crystals of apatite included in the groundmass suggests high rates of cooling and disequilibrium crystallization (Wyllie *et al.* 1962).

The composition of phillipsite-Na in the ijolitic pegmatites differs noticeably from the chemical compositions shown by Deer *et al.* (1962) and by Gottardi & Galli (1985). The  $SiO_2$ ,  $Al_2O_3$  and  $Na_2O$  contents are considerably higher than in other samples, and  $K_2O$ , BaO and CaO are only found as traces, resulting nearly in an end-member composition of the series defined by Coombs *et al.* (1997). The textural relationships that develop between the phillipsite-Na amygdules, the remaining minerals and the groundmass are also very significant. In some cases, they are scattered, with approximately ovoid shape, with an ocellus-like appearance in a matrix of devitrified glass (Fig. 3A). In others, the amygdules have been deformed and squeezed between pyroxene crystals, nepheline and groundmass in such a way that their surfaces develop folds generally occupied by the groundmass (Fig. 3D). It is highly improbable that this geometry is the result of deuteric fillings of small vesicular cavities, especially where they abound and where they are empty in the adjacent host-rock. Figure 3E also shows a textural relationship that is typical of liquid immiscibility between the devitrified groundmass and the amygdule (= *ocellus*) of phillipsite-Na. Values of  $\delta^{18}O$  for early-crystallizing phases (nepheline, clinopyroxene and magnetite) suggest a magmatic origin of the aqueous phase; even the isotopic composition of the earliest generation of calcite, which is the latest phase of the crystallization sequence after phillipsite-Na (Galliski *et al.* 1992), favors a juvenile origin for carbon and a deep crustal or mantle origin for  $H_2O$ . Consequently, they are interpreted as globules of melt separated by liquid immiscibility between the two phases.

Naslund (1976) experimentally proved that in the system  $KAlSi_3O_8 - NaAlSi_3O_8 - FeO - Fe_2O_3 - SiO_2$ , liquid immiscibility may proceed in a wide range of temperatures, and the dimension of the immiscibility field expands progressively with increasing  $f(O_2)$ . Philpotts (1971, quoted by Roedder 1979) found that mixtures of teschenite and its *ocelli*, composed of nepheline + analcime and run in an anhydrous state, did not show immiscibility, although it was developed at a low  $P(H_2O)$ , suggesting that  $H_2O$  favored the immiscibility process. Freestone (1978) showed that minor amounts of  $P_2O_5$  and  $TiO_2$  added to the system fayalite – leucite – silica expand the two-liquid field toward K-rich extremes. Thus, it might be possible that the concurrence of more than one of these factors led by high  $f(O_2)$  played a significant role in triggering the liquid-immiscibility process at low pressures.

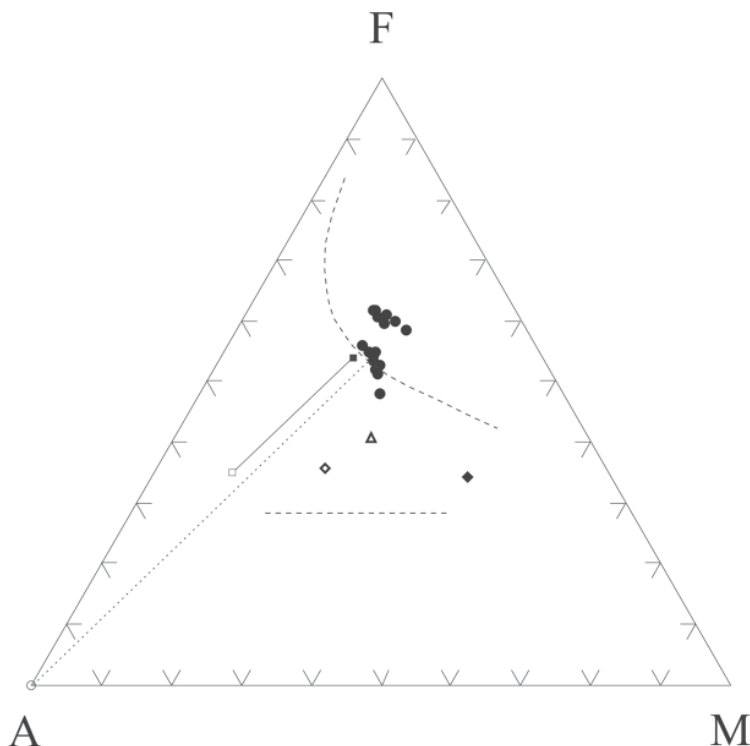


FIG. 23. Plot of A ( $\text{Na}_2\text{O} + \text{K}_2\text{O}$ ), F (FeO) and M (MgO), showing the compositions of the groundmass (solid circles) of the La Madera ijolitic pegmatites and the compositions of the phillipsite-Na (open circles) of the amygdules, linked through a dashed line. Solid diamond, open diamond and open triangle show the compositions of melanephelinite, ijolitic pegmatite and zeolite-bearing ijolitic pegmatite, respectively. Dashed lines outline approximately the interpreted field of immiscibility in the rocks of the Monteregian province, taken from Philpotts (1976); solid and open squares related by a tie-line represent the compositions of matrix and ocelli, respectively, in a sill of fourchite near Montreal, Quebec, studied by him.

The unmixing process between two different liquids has already been verified in fluid inclusions of apatite from some ijolitic pegmatites of Kenya (Rankin & Le Bas 1974). The quantitative chemical compositions could not be determined in this case, but one of the fractions in that situation is rich in silicates (brown glass), and the other is rich in carbonates.

At La Madera, the leucocratic fraction containing phillipsite-Na, minor apatite, calcite, opaque minerals and chlorite corresponds to the phase rich in carbonates, and the brown glass represents the more basic fraction. The chemical compositions of the phillipsite-Na and the groundmass show that the major elements underwent considerable partitioning, with Si, Al, Na, Ca and  $\text{CO}_3^{2-}$  concentrated in the light-colored phase, and Mg, Fe, K, P and Ti enriched in the more basic phase. The chemical composition of the groundmass and the phillipsite-Na were plotted in the AFM triangle (Fig. 23), where the immiscibility field found by Philpotts (1976) for the

compositions of matrix and the *ocelli* of rocks of the Monteregian province of Quebec is indicated. Almost all the compositions of the dark groundmass of the ijolitic pegmatites plot along the boundary line defined by the matrix studied by Philpotts (1976). The other points are shifted away from the line, closer to the F corner; following an almost parallel arrangement, they correspond to the compositions of the groundmass of the zeolite-bearing ijolitic pegmatites. The displacement is more a consequence of total alkali depletion than of Fe enrichment compared to the previous one. The compositions of the amygdules of the ijolitic pegmatites, which represent the equivalent of the *ocelli* of Philpotts (1976), plot exactly at the A corner of the AFM diagram because it only accounts for phillipsite-Na, the most abundant phase, whereas the subordinate amounts of chlorite, calcite and apatite are not considered. It is evident in the diagram that the compositions of the groundmass and amygdules of La Madera ijolitic

pegmatites parallel the compositions of the pairs groundmass–ocelli from the Monteregian rocks, and support the immiscibility interpretation from the chemical perspective. This interpretation finds additional support in the different concentrations of some trace elements in the ijolite dykelets and in those ijolites with zeolites, which would represent the rocks with the highest percentage of leucocratic component. In the dykelets, there is a higher concentration of Zr and Hf and lower Rb than in the leucocratic rocks.

The magmatic evolution of the ijolitic pegmatites can be schematically portrayed in the pseudoternary system diopside – nepheline – apatite studied by Kogarko *et al.* (1984). An olivine melanephelinitic magma evolves by crystallization of those three phases after resorbing initial olivine and melilite to compositions with an increasing apatitic index as it differentiates from ijolite to an urtite. In the La Madera magmas, however, the predominant crystallization of nepheline and its later transformation into albite with increasing  $a\text{SiO}_2$  did not take place owing to the  $\text{H}_2\text{O}$  enrichment in the remaining melt. Instead, it proceeded to the field of liquid immiscibility, and phillipsite-Na is directly formed as a phase rich in Na, Al and  $\text{H}_2\text{O}$ , suggesting that the residual liquid was close in composition to nepheline syenite.

The integrated analysis of the previous discussion permits the establishment of the following successive stages of pegmatite development: (1) The thermal contrasts between the already consolidated host-rock of olivine melanephelinite composition and the injected pegmatite-forming melt triggered the crystallization of pyroxene, nepheline, apatite, perovskite and magnetite. The process probably occurred in a  $\text{H}_2\text{O}$ -undersaturated alkali-enriched melt with high activities of  $\text{PO}_4^{3-}$  and  $\text{CO}_3^{2-}$ , generating conditions that provoked low viscosity, inhibition of nucleation and high rates of crystal growth under a definite thermal gradient. (2) In very localized domains at the tops of some dykelets or in some segregation vesicles, there was an increase in  $\text{H}_2\text{O}$  concentration causing analcime to form as a primary mineral. (3) The path of crystallization evolved toward an enrichment of volatiles and incompatible elements in the melt, until the immiscibility between two fractions occurred. One of these fractions is represented by the devitrified glass of the groundmass or by the brown glass of the segregation vesicles. It has a composition comparatively impoverished in Na, Al and Ca, and enriched in Mg, Fe, K, and P that crystallizes as abundant acicular late-stage fluorapatite. The other phase is represented by the amygdules with phillipsite-Na, minor apatite, carbonates, chlorite and Fe oxides, and is rich in Si, Al, Na, and Ca. The relative volumes of both phases vary, and the leucocratic phase crystallized as the amygdule-filling minerals or was segregated with part of the dark phase to form the ijolitic pegmatites with zeolites. (4) The progressive enrichment in  $\text{H}_2\text{O}$  in the residual melt lowered the solidus temperature and inhibited crystallization to produce a glass. (5) In the lat-

est stages of glass solidification at subsolidus conditions, and probably in the presence of an active gaseous phase, alkali-enriched amphiboles and biotite crystallized as coronas around magnetite and the unidentified mineral with the star-shaped habit. (6) The composition of the dark immiscible phase of the ijolitic pegmatites does not exactly correspond to any common rock, but it is close in Si, Fe, Mg and Ti to the contents of a basanite and plots within this field in the TAS diagram. The equivalent composition of the dark immiscible phase in the ijolitic pegmatites with zeolites plots slightly displaced with respect to the field of the alkali basalts. The composition of the light immiscible fraction is similar in terms of major elements to those of a nepheline syenite plus a small percentage of carbonatite. (7) Consequently, the association of nepheline syenites and carbonatites in ijolite – nepheline syenite – carbonatite alkaline complexes may not originate by extreme magmatic differentiation, but instead may represent immiscible melts that unmix at specific moments of the evolution of the magmatic system.

#### CONCLUSIONS

1. The ijolitic pegmatites of La Madera constitute dykes and dykelets formed by crystallization of evolved melts derived through fractional crystallization of the magma that formed the olivine melanephelinite host-rock.
2. The pegmatites were emplaced and crystallized preferentially above or, with a lower frequency of incidence, at the upper cooling front of the lava pond.
3. The development of the pegmatitic texture was initiated because the comparative enrichment of the melt in flux components ( $\text{PO}_4^{3-}$ ,  $\text{CO}_3^{2-}$ ,  $\text{CO}_2$ ,  $\text{H}_2\text{O}$ , ) inhibited nucleation, diminished the viscosity of the fluid and favored an increasing rate of disequilibrium crystal-growth.
4. During the evolution of the system, the remaining melt separated into two immiscible fractions, with major-element compositions that are similar to those of a nepheline syenite with a discrete carbonatite component in one fraction, and somewhat similar to that of a basanite and alkali basalt in the other.

#### ACKNOWLEDGEMENTS

Field work and laboratory studies were partially supported by CONICET grants PIP 349/89 and 319/98 of to MAG, who gratefully acknowledges the field and lab assistance of M.F. Márquez-Zavalía, J. Oyarzábal, and the XRD patterns obtained by G. Mas. RL deeply appreciates the assistance of Drs. Edward Ripley, Insung Lee, Timothy Johnson and Steve Studley at Indiana University. The reviews of D. London, P. Tice, J. Nizamoff and A.U. Falster considerably improved this paper, as well as the editorial corrections and suggestions of W.B. Simmons Jr. and especially of R.F. Martin.

## REFERENCES

- ANDERSON, A.T., JR., SWIHART, G.H., ARTIOLI, G. & GEIGER, C.A. (1984): Segregation vesicles, gas filter-pressing, and igneous differentiation. *J. Geol.* **92**, 55-72.
- BAILEY, D.K. & HAMPTON, C.M. (1990): Volatiles in alkaline magmatism. *Lithos* **26**, 157-165.
- BOTTINGA, Y. & JAVOY, M. (1973): Comments on oxygen isotope geothermometry. *Earth Planet. Sci. Lett.* **20**, 250-265.
- \_\_\_\_\_ & \_\_\_\_\_ (1975): Oxygen isotope partition among the minerals in igneous and metamorphic rocks. *Rev. Geophys. Space Phys.* **13**, 401-418.
- CHAKHMOURADIAN, A.R., REGUIR, E.P. & MITCHELL, R.H. (2002): Strontium-apatite: new occurrences and the extent of Sr-for-Ca substitution in apatite-group minerals. *Can. Mineral.* **40**, 121-136.
- CLAYTON, R.N. & MAYEDA, T.K. (1963): The use of bromine pentafluoride in the extraction of oxygen from oxides and silicates for isotopic analysis. *Geochim. Cosmochim. Acta* **27**, 43-52.
- COOMBS, D.S., ALBERTI, A., ARMBRUSTER, T., ARTIOLI, G., COLELLA, C., GALLI, E., GRICE, J.D., LIEBAU, F., MANDARINO, J.A., MINATO, H., NICKEL, E.H., PASAGLIA, E., PEACOR, D.R., QUARTIERI, S., RINALDI, R., ROSS, M., SHEPPARD, R.A., TILLMANN, S. & VEZZALINI, G. (1997): Recommended nomenclature for zeolite minerals: report of the Subcommittee on Zeolites of the International Mineralogical Association, Commission on New Minerals and Mineral Names. *Can. Mineral.* **35**, 1571-1606.
- DEER, W.W., HOWIE, R.A. & ZUSSMAN, J. (1962): *Rock-Forming Minerals. 5. Non-silicates*. Longman, London, U.K.
- FENN, P.M. (1977): The nucleation and growth of alkali feldspars from hydrous melts. *Can. Mineral.* **15**, 135-161.
- FREESTONE, I.C. (1978): Liquid immiscibility in alkali-rich magmas. *Chem. Geol.* **23**, 115-123.
- GALLISKI, M.A. & LIRA, R. (1991): Hallazgo de un nuevo afloramiento de foiditas en la región de Chaján, provincia de Córdoba. Unpublished report.
- \_\_\_\_\_, \_\_\_\_\_ & OYARZÁBAL, J.C. (1992): Los pegmatoides foidíferos del Cerro La Madera, provincia de Córdoba: mineralogía y paragénesis. *Actas I Reunión de Mineralogía y Metalogénesis* **2**, 393-404.
- GOTTARDI, G. & GALLI, E. (1985): *Natural Zeolites*. Springer-Verlag, Berlin, Germany.
- GREENOUGH, J.D. & DOSTAL, J. (1992): Layered rhyolite bands in a thick North Mountain Basalt flow: the products of silicate liquid immiscibility? *Mineral. Mag.* **56**, 309-318.
- HAGGERTY, S.E. (1976): Opaque mineral oxides in terrestrial igneous rocks. In *Oxide Minerals* (D. Rumble III, ed.). *Rev. Mineral.* **8**, 101-300.
- HAMILTON, D.L. (1961): Nephelines as crystallization temperatures indicators. *J. Geol.* **69**, 321-329.
- HELZ, R.T. (1980): Crystallization history of Kilauea Iki lava lake as seen in drill core recovered in 1967-1979. *Bull. Volcanol.* **43**, 675-701.
- \_\_\_\_\_, KIRSCHENBAUM, H. & MARINENKO, J.W. (1989): Diapiric transfer of melt in Kilauea Iki lava lake, Hawaii: a quick, efficient process of igneous differentiation. *Geol. Soc. Am., Bull.* **101**, 578-594.
- HOEFS, J. (1987): *Stable Isotope Geochemistry* (3<sup>rd</sup> ed.). Springer-Verlag, Heidelberg, Germany.
- JAHNS, R.H. & BURNHAM, C.W. (1969): Experimental studies of pegmatite genesis. I. A model for the derivation and crystallization of granitic pegmatites. *Econ. Geol.* **64**, 843-864.
- KJARSGAARD, B.A. & HAMILTON, D.L. (1988): Liquid immiscibility and the origin of alkali-poor carbonatites. *Mineral. Mag.* **52**, 43-55.
- KOGARKO, L.N. (1990): Ore-forming potential of alkaline magmas. *Lithos* **26**, 167-175.
- \_\_\_\_\_, KRIGMAN, L.D. & BELYAKOVA, N.Y. (1984): The nepheline - diopside - apatite system and liquid evolution during the crystallization of an apatite-bearing ijolite-urtite magma. *Geochem. Int.* **21**, 38-58.
- KONONOVA, V.A., ORGANOVA, N.I. & LOMEYKO, Y.I. (1967): Composition and crystallization temperature of nepheline from rocks of an ijolite-melteigite series. *Int. Geol. Rev.* **9**, 1229-1236.
- KOSTER VAN GROOS, A.F. & WYLLIE, P.J. (1968): Liquid immiscibility in the join NaAlSi<sub>3</sub>O<sub>8</sub>-Na<sub>2</sub>CO<sub>3</sub>-H<sub>2</sub>O and its bearing on the genesis of carbonatites. *Am. J. Sci.* **266**, 932-967.
- KUNO, H. (1965): Fractionation trends of basalt magmas in lava flows. *J. Petrol.* **6**, 302-321.
- \_\_\_\_\_, YAMASAKI, K., IIDA, C. & NAGASHIMA, K. (1957): Differentiation of Hawaiian magmas. *Jap. J. Geol. Geography* **28**, 179-218.
- LEAKE, B.E. (1978): Nomenclature of amphiboles. *Can. Mineral.* **16**, 501-520.
- \_\_\_\_\_, WOOLLEY, A.R., ARPS, C.E.S., BIRCH, W.D., GILBERT, M.C., GRICE, J.D., HAWTHORNE, F.C., KATO, A., KISCH, H.J., KRIVOVICHEV, V.G., LINTHOUT, K., LAIRD, J., MANDARINO, J.A., MARESCHE, W.V., NICKEL, E.H., ROCK, N.M.S., SCHUMACHER, J.C., SMITH, D.C., STEPHENSON, N.C.N., UNGARETTI, L., WHITTAKER, E.J.W. & GUO, YOUZHI (1997): Nomenclature of amphiboles: report of the Subcommittee on Amphiboles of the International Mineralogical Association, Commission on New Minerals and Mineral Names. *Can. Mineral.* **35**, 219-246.
- LE BAS, J.M. (1977): *Carbonatite-Nephelinite Volcanism*. John Wiley & Sons, London, U.K.

- \_\_\_\_\_ (1989): Nephelinitic and basanitic rocks. *J. Petrol.* **30**, 1299-1312.
- \_\_\_\_\_ & HANDLEY, C.D. (1979): Variation in apatite composition in ijolitic and carbonatitic igneous rocks. *Nature* **279**, 54-56.
- LE MAITRE, R.W., ed. (2002): *Igneous Rocks: a Classification and Glossary of Terms* (2<sup>nd</sup> ed.). Cambridge University Press, Cambridge, U.K.
- LINDSLEY, D.H., SMITH, D. & HAGGERTY, S.E. (1971): Petrography and mineral chemistry of a differentiated flow of Picture Gorge Basalt near Spray, Oregon. *Carnegie Inst. Wash. Yearbook* **69**, 264-285.
- LONDON, D. (1992): The application of experimental petrology to the genesis and crystallization of granitic pegmatites. *Can. Mineral.* **30**, 499-540.
- \_\_\_\_\_, MORGAN, G.B., IV & HERVIG, R.L. (1989): Vapor-undersaturated experiments with Macusani glass + H<sub>2</sub>O at 200 MPa, and the internal differentiation of granitic pegmatites. *Contrib. Mineral. Petrol.* **102**, 1-17.
- LOPEZ, M.G. & SOLÁ, P. (1981): Manifestaciones volcánicas alcalinas de los alrededores de Las Chacras y de la región de Villa Mercedes-Chaján, Provincias de San Luis y Córdoba. *VIII Cong. Geol. Arg. Actas* **IV**, 967-978.
- MCDONOUGH, W.F. & SUN, S.-S. (1995): The composition of the Earth. *Chem. Geol.* **120**, 223-253.
- McMILLAN, K., CROSS, R.W. & LONG, P.E. (1987): Two-stage vesiculation in the Cohasset flow of the Grande Ronde Basalt, south-central Washington. *Geology* **15**, 809-812.
- MOGESSIE, A. & TESSADRI, R. (1982): A basic computer program to determine the name of an amphibole from an electron microprobe analysis. *Geol. Paläont. Mitt.* **II**, 7, 259-289.
- \_\_\_\_\_, \_\_\_\_\_, & VELTMAN, C.B. (1990): EMP-AMPH: a hypercard program to determine the name of an amphibole from electron microprobe analysis according to the International Mineralogical Association scheme. *Comput. & Geosci.* **16**, 309-330.
- MORIMOTO, N. (1988): Nomenclature of pyroxenes. *Mineral. Petrol.* **39**, 55-76.
- NASLUND, H.R. (1976): Liquid immiscibility in the system KAlSi<sub>3</sub>O<sub>8</sub>-NaAlSi<sub>3</sub>O<sub>8</sub>-FeO-Fe<sub>2</sub>O<sub>3</sub>-SiO<sub>2</sub> and its application to natural magmas. *Carnegie Inst. Wash., Yearb.* **75**, 592-597.
- OHMOTO, H. (1972): Systematics of sulfur and carbon isotopes in hydrothermal ore deposits. *Econ. Geol.* **67**, 551-578.
- PHILPOTTS, A.R. (1971): Immiscibility between feldspathic and gabbroic magmas. *Nature* **229**, 107-109.
- \_\_\_\_\_ (1976): Silicate liquid immiscibility: its probable extent and petrogenetic significance. *Am. J. Sci.* **276**, 1147-1177.
- POUCHOU, J.L. & PICOIR, F. (1985): "PAP" (φ-ρ-z) procedure for improved quantitative microanalysis. In *Microbeam Analysis* (J.T. Armstrong, ed.). San Francisco Press, San Francisco, California (104-106).
- PUFFER, J.H. & HORTER, D.L. (1993): Origin of pegmatitic segregation veins within flood basalts. *Geol. Soc. Am., Bull.* **105**, 738-748.
- RANKIN, A.H. & LE BAS, M.J. (1974): Liquid immiscibility between silicate and carbonate melts in naturally occurring ijolite magma. *Nature* **250**, 206-209.
- ROCK, N.M.S. & LEAKE, B.E. (1984): The International Mineralogical Association amphibole nomenclature scheme: computerization and its consequences. *Mineral. Mag.* **48**, 211-227.
- ROEDDER, E. (1979): Silicate liquid immiscibility in magmas. In *The Evolution of Igneous Rocks, Fiftieth Anniversary Perspectives* (H.S. Yoder Jr., ed.). Princeton University Press, Princeton, New Jersey (15-57).
- ROSENBAUM, J. & SHEPPARD, S.M.F. (1986): An isotopic study of siderites, dolomites, and ankerites at high temperatures. *Geochim. Cosmochim. Acta* **50**, 1147-1150.
- RYE, R.O. & OHMOTO, H. (1974): Sulfur and carbon isotopes and ore genesis. A review. *Econ. Geol.* **69**, 826-842.
- SCHAIRER, J.F. & YODER, H.S., JR. (1962): Pyroxenes: the system diopside - enstatite - silica. *Carnegie Inst. Wash., Yearb.* **62**, 75-82.
- SMITH, R.E. (1967): Segregation vesicles in basaltic lava. *Am. J. Sci.* **265**, 696-713.
- TAYLOR, B.E. (1987): Stable isotope geochemistry of ore-forming fluids. In *Stable Isotope Geochemistry of Low Temperature Fluids* (T.K. Kyser, ed.). *Mineral. Assoc. Can., Short Course Handbook* **13**, 337-445.
- TILLEY, C.E. (1954): Nepheline - alkaline feldspars paragenesis. *Am. J. Sci.* **252**, 65-75.
- VEKSLER, I.V. & TEPTILEV, M.P. (1990): Conditions for crystallization and concentration of perovskite-type minerals in alkaline magmas. *Lithos* **26**, 177-189.
- WYLLIE, P.J., BAKER, M.B. & WHITE, B.S. (1990): Experimental boundaries for the origin and evolution of carbonatites. *Lithos* **26**, 3-19.
- \_\_\_\_\_, COX, K.G. & BIGGAR, G.M. (1962): The habit of apatite in synthetic systems and igneous rocks. *J. Petrol.* **3**, 238-243.

Received July 18, 2003, revised manuscript accepted September 23, 2004.